Title
KRAS Expands and Exhausts Hematopoietic Stem Cells

Author
Sasine, Joshua P

Publication Date
2018

Peer reviewed|Thesis/dissertation

UNIVERSITY OF CALIFORNIA

Los Angeles

KRAS Expands and Exhausts Hematopoietic Stem Cells

A dissertation submitted in partial satisfaction of the requirements for the degree Doctor of Philosophy in Molecular, Cellular, and Integrative Physiology

by

Joshua Parks Sasine

2018

ABSTRACT OF THE DISSERTATION

KRAS Expands and Exhausts Hematopoietic Stem Cells

by

Joshua Parks Sasine

Doctor of Philosophy in Molecular, Cellular, and Integrative Physiology

University of California, Los Angeles, 2018

Professor John P. Chute, Chair

Expressing the oncogenic mutant form of *Kras* in hematopoietic stem cells (HSCs) induces a rapidly fatal myeloproliferative neoplasm in mice, suggesting *Kras* signaling plays a dominant role in normal hematopoiesis. However, the oncogenic mutant is insensitive to signal-terminating GTPase-activating proteins, resulting in unabated signal which is not encountered in normal physiology. Hence, we sought to determine the effect of simply increasing the amount of endogenous wild-type *Kras* on HSC fate. To this end, we utilized a codon-optimized version of the murine Kras gene (Kras ex3op), in which silent mutations in exon 3 render

the encoded mRNA more efficiently translated, leading to increased protein expression without disruption to the normal gene architecture. We found that KRAS protein levels were significantly increased in bone marrow (BM) HSCs in *Kras* $^{ex3op/ex3op}$ mice, demonstrating that the translation of KRAS in HSCs is normally constrained by rare codons. *Kras* $^{ex3op/ex3op}$ mice displayed expansion of BM HSCs, progenitor cells and B lymphocytes, but no evidence of myeloproliferative disease or leukemia in mice followed for 22 months. BM HSCs from *Kras*$^{ex3op/ex3op}$ mice demonstrated increased multilineage repopulating capacity in primary competitive transplantation assays, but secondary competitive transplants revealed exhaustion of long-term HSCs. Following total body irradiation, *Kras*$^{ex3op/ex3op}$ mice displayed accelerated hematologic recovery and increased survival. Mechanistically, HSCs from *Kras*$^{ex3op/ex3op}$ mice demonstrated increased proliferation at baseline, with a corresponding increase in ERK1/2 phosphorylation and CDK4/6 activation. Furthermore, both the enhanced colony forming capacity and in vivo repopulating capacity of HSCs from *Kras*$^{ex3op/ex3op}$ were dependent on CDK4/6 activation. Finally, BM transplantation studies revealed that augmented KRAS produced expansion of HSCs, progenitor cells and B cells in a hematopoietic cell-autonomous manner, independent from effects on the BM microenvironment. This study provides fundamental demonstration of codon usage in a mammal having a biological consequence.

The dissertation of Joshua P. Sasine is approved.

Dinesh Subba Rao

Gay M. Crooks

Kenneth A. Dorshkind

John P. Chute, Committee Chair

University of California, Los Angeles

2018

Table of Contents

Acknowledgements

I would like pay sincere gratitude to my advisor Dr. John Chute. His broad knowledge on the basic biology and clinical practice imparted a unique and enriching training experience. He provided an environment with more than sufficient resources to accomplish the work. Dr. Chute has been a mentor and advocate in every respect, allowing me the freedom to explore my ideas while providing guidance and direction when it's needed most.

I would also like to express my gratitude to the members of my committee at UCLA: Dr. Dinesh Rao, Dr. Gay Crooks and Dr. Ken Dorshkind. They provided insightful comments which enriched the depth of the project.

I was also fortunate to have worked with a group of talented and collegial team within the Chute lab. Among them, Dr. Heather Himburg, Dr. Martina Roos, Dr. Tina Termini, and Dr. Mamle Quarmyne provided essential mentorship, discussion of the experimental results, and technical expertise.

Because I was a clinical fellow in hematology and medical oncology, I had access to a doctoral degree program only through the Specialty Training and Advanced Research Program (STAR). This revolutionary organization is led by Dr. Linda Demer and Dr. Mitch Wong and backed by the Chair of the Department of Medicine, Dr. Alan Fogelman. I am sincerely grateful for their leadership, mentorship, and drive to continue this program. Without them, this path would not have been possible.

I also thank my funding sources: the National Institutes of Health Training Grant, the Broad Stem Cell Research Center at UCLA, the American Society of Clinical Oncology, and the Tower Cancer Research Foundation.

PREFACE

This work was directly supported by a National Institutes of Health Training Grant, 4T32HL066992-14 (MPI), awarded to the Division of Hematology-Oncology, University of California, Los Angeles. It was also supported by the California Institute of Regeneration Medicine and the Eli and Edythe Broad Center of Regenerative Medicine and Stem Cell Research Center Clinical Fellow Training Program.

This work has been previously published and any reproductions here are with permission of the journal: Sasine JP, Himburg HA, Termini CM, Roos M, Tran E, Zhao L, Kan J, Li M, Zhang Y, de Barros SC, Rao DS, Counter CM, Chute JP. Wild-type Kras expands and exhausts hematopoietic stem cells. JCI Insight. 2018 Jun 7;3(11).

Vita

Education

2001 – 2004 **University of Northern Colorado**, Bachelor of Science

2007 – 2011 **University of Miami Leonard M. Miller School of Medicine**, Doctor of Medicine

Clinical Training

2011–2013 **University of California, Los Angeles**, Internal Medicine Internship and Residency

2013–2016 **University of California, Los Angeles**, Hematology-Oncology Fellowship

2016–2017 **University of California, Los Angeles**, Advanced Hematopoietic Cell Transplant Fellowship

PROFESSIONAL EXPERIENCE

2003 Undergraduate Researcher, University of Colorado Health Science Center

2005 – 2007 Research Laboratory Technician, University of Utah, Salt Lake City, UT

2007 – 2011 Medical Student, University of Miami, FL

2011 – 2013 Internal Medicine Resident, ABIM Research Pathway, UCLA, Los Angeles, CA

2013 – 2016 Hematology/Oncology Fellow, ABIM Research Pathway, UCLA

2014 – STAR Fellow and PhD Candidate, UCLA, Los Angeles, CA

2016 – 2017 Advanced Hematopoietic Cell Transplant Fellow, UCLA, Los Angeles, CA

2017 – Clinical Instructor, UCLA

2017 – Medical Director, CAR T-Cell Program, UCLA

AWARDS & HONORS

2001-2004	Dean's List – all 7 semesters
2004	Cum Laude Graduate
2007 – 2011	University of Miami School of Medicine Merit-Based Scholarship
2011	University of Miami School of Medicine Service Award
2012	UCLA Commendations for Excellence in Medical Student Teaching Award
2013 –	American Board of Internal Medicine Research Pathway Designation
2013	UCLA STAR (Specialty Training and Advanced Research) Program Award
2015 – 2017	Eli & Edythe Broad Center of Regenerative Medicine & Stem Cell Research at UCLA Clinical Fellow Training Program Award
2017	UCLA Department of Medicine, Specialty Training and Advanced Research Innovator Award
2017 – 2018	Chief Fellow, UCLA STAR Program
2017 – 2018	ASCO Young Investigator Award
2017 – 2019	Tower Cancer Research Foundation Career Development Award

Chapter 1

Introduction

Introduction

The mammalian Ras family is composed of 3 genes that encode 4 small GTPase proteins that regulate cell fate[1-4]: HRAS, NRAS, KRAS4A, and KRAS4B. RAS proteins transmit signals from surface receptors to intracellular signaling proteins[1-4]. RAS proteins share 79% amino acid sequence identity, with variability residing in the last 25 amino acids that encode sites of posttranslational modifications[5]. Each Ras gene has identical effector binding domains but important differences lie in their unique posttranslational modifications which confer dissimilar trafficking routes resulting in distinct plasma membrane microdomain localization[6]. As a result, they have access to different effector pools and are capable of generating distinct signal outputs[7]. Activation of KRAS, more than NRAS or HRAS, is able to confer stem-like properties[8]. Additionally, KRAS, but not NRAS or HRAS, is upregulated in activated stem cells and progenitors compared to HSCs[9], and in pre-leukemic states such as DNMT3A or TET2 knockout[10]. Mice lacking functional HRAS and/or NRAS are viable[11], whereas those lacking KRAS die during embryogenesis but are rescued by substitution of HRAS into the KRAS locus[12], emphasizing that that although their unique intrinsic protein properties are important, differential regulation of expression is the ultimate determination of their relative significance.

RAS proteins alternate between GTP- (activate) and GDP-bound (inactive) conformations. Substitution mutations can produce "oncogenic" forms which prevent the intrinsic and GAP (GTPase-Activating Proteins) catalyzed hydrolysis of GTP, thereby generating overactive RAS that can chronically activate effector pathways[13]. The consequences of GAP-responsive wild-type Ras protein overexpression in the hematopoietic system at steady-state were previously unknown since current understanding of the role of RAS signaling in the hematopoietic system has been

driven primarily by studies in which oncogenic mutant Ras transgenes were expressed (or overexpressed)[14,15] in bone marrow (BM) hematopoietic stem cells (HSCs) and progenitor cells[16-24]. These various methods to introduce oncogenic mutant RAS proteins into the hematopoietic system have not yielded consistent consequences. Bone marrow hematopoietic stem cell (HSC) numbers have been increased or decreased[16,20] and variable effects on malignancy genesis were observed (T-cell leukemia[18], B-lymphoblastic leukemia/lymphoma[14], myeloid leukemia/myeloproliferative diseases[16,18,19], or none[20]). This might be due, in part, to differences in RAS protein levels. The expression level of oncogenic NRAS is significantly correlated with likelihood of causing a AML vs CMML in mice[25] and both the oncogenic and wild-type forms are commonly overexpressed in human AML[26,27]. Critically, expression of oncogenic NRAS at physiologic levels is not sufficient to produce leukemia[19,28]. The genomic region harboring the KRAS1P pseudogene is amplified in a variety of human cancers and can act as a competing endogenous RNA decoy to upregulate the wild-type KRAS protein[29,30]. However, this new field has not addressed what effects, if any, result from overexpression of GAP-responsive wild-type Ras proteins on leukemic or normal HSCs.

Transducing oncogenic HRAS into hematopoietic stem/progenitor cells (HSPCs) in combination with pharmacologic RAS pathway antagonism increased proliferation and frequency of progenitors with enhanced self-renewal capacity[15]. Thus, a moderate increase of RAS activity augmented stem cell features of HSCs. KRAS and ERK1/2 are required for hematopoiesis[31,32] and our prior work showed that the effect of pleiotrophin, a growth factor for HSCs, occurs, at least in part, through activation of the RAS pathway, further supporting the importance of RAS in HSC regulation[33-35].

These findings highlight the importance of RAS protein activation in HSCs. However, a difference exists between oncogenic RAS proteins, often overexpressed, chronically driving high levels of signaling and the wild-type, GAP-responsive versions. Overexpressing the wild-type version might have distinct consequences and has not been directly tested in hematopoiesis.

In order to directly test this hypothesis, we utilized a version of the *Kras* gene that generates higher levels of the wild-type KRAS protein by virtue of increased translation without altering the normal gene architecture. More specifically, we utilized the $Kras^{ex3op}$ gene, which was created by introducing 33 silent mutations into exon 3 of the endogenous *Kras* gene to change 27 rare codons to their common counterparts to optimize translation; this produces a 2- to 4-fold increase in KRAS protein compared with the unaltered allele[1] (**Figure 1**). Although the amino acid sequences of Ras genes are highly similar, the nucleotide sequences are more divergent, with *Kras* preferentially encoded by A or T at wobble base pairs, whereas *Hras* is encoded by G or C, and *Nras* by a mixture of all 4 nucleotides[1,36]. Codons ending in A or T are rare in mammalian exomes and rare codons have been shown to impede the efficiency of translation elongation[1,37]. Consistent with this, the rare codons in *Kras* have been shown to impede translation of the encoded mRNA, reducing protein expression[1,36].

We show here that a mere 2-fold increase in the amount of wild-type KRAS, which retains GAP responsiveness, in the hematopoietic compartment led to an increase in HSC proliferation and short-term repopulating capacity as measured in primary competitive transplantation assays, while substantially improving hematopoietic regeneration and survival in mice following high-dose

irradiation. However, these positive effects ultimately led to the exhaustion of long-term HSCs (LT-HSCs), as measured in competitive secondary transplantation assays. Taken together, these results reveal the nuanced physiologic function of wild-type KRAS in regulating HSC fate and suggest that augmentation of KRAS signaling has therapeutic potential for the immediate management of myelosuppression. Moreover, this study demonstrates that codon usage in a mammal has biological consequences, which speaks to the importance of codon usage in mammalian biology.

Chapter 2

Results

KRAS is abundance increases with maturation of hematopoietic stem cells into progenitor stages

To understand how the abundance of KRAS protein is regulated in the hematopoietic system at steady-state in vivo, we used intracellular flow cytometry on mouse hematopoietic cell subsets and found that high expression is correlated with activated progenitor populations, especially myeloid progenitor populations. HSCs have a comparatively low level of KRAS protein (**Figure 2**). This is consistent with recent data showing that unlike *Nras* or *Hras*, expression of *Kras* mRNA is higher in activated HSCs (non label-retaining) and multipotent progenitors (MPPs) compared to dormant HSCs (label-retaining, 2.5 fold, p=0.0005)[9].

While this association of KRAS with hematopoietic maturation has been previously described, whether it is a causal association is unknown. HSCs are characterized (among others) as mainly quiescent and rare. We wondered if driving increased levels of KRAS in HSCs is sufficient to force the HSCs into the progenitor stages or confer some features of progenitors upon the HSCs. We also wondered if this would be sufficient for oncogenesis given the known effects of oncogenic mutant KRAS. Additionally, there is evidence that overexpression of KRAS might be correlated with tumorigenesis. KRAS1P is an expressed pseudogene which competes with the KRAS mRNA for mircroRNA binding. Amplification of KRAS1P can sponge up microRNA which would normally negatively regulate KRAS and thereby increase abundance of KRAS mRNA and this phenomenon is seen in several human cancers[29,38]. However, other evidence would suggest that wild-type KRAS is tumor suppressive. Loss of wild-type *Kras* activates all Ras isoforms in experimental models of leukemogenesis and produces a more aggressive form of leukemia in

mice[39]. Overexpression of KRAS has been shown to protect mice against lung carcinogenesis and lung cancers arising from KRAS overexpressing cells are smaller and less invasive[1].

To test the consequences of KRAS overexpression in the hematopoietic system *in vivo*, we utilized the aforementioned unique genetic model, the *Kras*$^{ex3op/ex3op}$ mouse[1] which exploits the rare codon bias that limits KRAS translation. By making 33 synonymous mutations which common codon usage without altering protein sequence, there is a 2 – 4 fold increase of the protein with no abnormal splice variants, no overt developmental phenotype, and normal lifespans[1].

Translation of KRAS protein in BM HSCs is constrained by rare codons

We sought to determine the effect of increased KRAS protein levels on HSC fate. We measured KRAS protein levels in BM ckit^{+}sca1^{+}lin^{-} (KSL) hematopoietic stem/progenitor cells (HSPCs) and CD150^{+} CD48^{-} KSL HSCs from *Kras*$^{ex3op/ex3op}$ mice versus mice expressing native *Kras* (*Kras*$^{nat/nat}$ mice). *Kras*$^{ex3op/ex3op}$ mice displayed significantly increased percentages of KRAS^{hi} KSL cells and KRAS^{hi} HSCs compared with control *Kras*$^{nat/nat}$ mice (**Figure 3**), confirming that the replacement of rare codons with common codons in exon 3 of *Kras* does indeed increase KRAS protein levels in the HSC and progenitor populations. Of note, the relative levels of KRAS protein were increased in BM KSL progenitor cells compared with BM HSCs in both *Kras*$^{ex3op/ex3op}$ mice and *Kras*$^{nat/nat}$ mice, consistent with prior studies demonstrating that protein translation overall is higher in progenitor cells than in HSCs[40].

***Kras*$^{ex3op/ex3op}$ mice display lymphocytosis and expansion of CD19^{+} B cells**

Hematologic analysis of *Kras*$^{ex3op/ex3op}$ mice and *Kras*$^{nat/nat}$ mice revealed an increase in peripheral blood white blood cells (PB WBCs) and lymphocytes in *Kras*$^{ex3op/ex3op}$ mice compared with control mice (**Figure 4**), whereas no differences in neutrophils, hemoglobin, or platelet counts were observed. Flow cytometric analysis of PB lymphocyte subsets demonstrated that the lymphocytosis was caused by an increase in CD19^{+} B cells (**Figure 4**). We observed no differences in the numbers of PB CD3^{+}, CD4^{+}, or CD8^{+} T cells and no differences in PB natural killer (NK) cells, naive T cells, or memory T cells (**Figure 4**). Analysis of percentages of T cell subsets in the thymus of 8-week-old *Kras*$^{ex3op/ex3op}$ mice and control mice also revealed no differences in T cell subsets or progenitors (**Figure 5**).

Finally, BM analysis revealed increased BM cell counts in *Kras*$^{ex3op/ex3op}$ mice compared with *Kras*$^{nat/nat}$ mice at baseline, but no differences were observed in the percentages of BM common lymphoid progenitor cells (CLPs), myelo-erythroid progenitor cells (MEPs), or granulocyte monocyte progenitor cells (GMPs) (**Figure 6**). A small increase in the percentage of BM common myeloid progenitor cells (CMPs) was observed in *Kras*$^{ex3op/ex3op}$ mice (**Figure 6**). We observed no differences in spleen mass between *Kras*$^{ex3op/ex3op}$ mice and *Kras*$^{nat/nat}$ mice (**Figure 6**).

Kras$^{ex3op/ex3op}$ mice do not develop myeloproliferative disease or leukemia

Since mice expressing oncogenic versions of either *Kras* or *Nras* develop myeloproliferative disease or hematologic cancers over time, we sought to determine whether increasing levels wild-type KRAS protein would similarly promote myeloid disease evolution. *Kras*$^{ex3op/ex3op}$ mice did

not develop myeloproliferative disease or myelodysplasia and no splenomegaly was observed through 20 months of age (**Figure 7**). Detailed immunophenotypic analysis also suggested no myeloid or lymphoid skewing at 20 months of age (**Figure 7**). We also did not observe gross changes in the BM microenvironment in *Kras*$^{ex3op/ex3op}$ mice over time (**Figure 8**). Lastly, we detected no germline mutations by Sanger sequencing in *Kras*, *Hras*, or *Nras* in *Kras*$^{ex3op/ex3op}$ mice to account for the observed hematopoietic phenotype in young adult mice.

Kras$^{ex3op/ex3op}$ mice display HSC expansion and exhaustion of long-term repopulating HSCs

Kras$^{ex3op/ex3op}$ mice displayed increased percentages and numbers of BM KSL cells and phenotypic HSCs compared with *Kras*$^{nat/nat}$ mice (**Figure 9**). *Kras*$^{ex3op/ex3op}$ mice also contained increased numbers of BM colony-forming cells (CFCs) and long-term culture–initiating cells (LTC-ICs) compared with control mice (**Figure 9**). Taken together, these results suggested that increased KRAS protein expanded both phenotypic HSCs and progenitor cells.

We next performed competitive repopulation assays to determine if *Kras*$^{ex3op/ex3op}$ mice contained increased functional HSC content. For this purpose, *Kras*$^{ex3op/ex3op}$ and *Kras*$^{nat/nat}$ mice were backcrossed more than 10 generations into C57BL/6 mice (CD45.2^{+}) and we utilized syngeneic recipient B6.SJL mice (CD45.1^{+}) as recipients. Recipient mice transplanted competitively with 2 $\times$ 10^{5} BM cells (CD45.2^{+}) from *Kras*$^{ex3op/ex3op}$ mice, along with 2 $\times$ 10^{5} competitor (CD45.1^{+}) BM cells, displayed significantly increased total donor CD45.2^{+} cell engraftment over time compared with mice transplanted with an equal dose of BM cells from *Kras*$^{nat/nat}$ mice. Recipient mice

transplanted with BM cells from *Kras*$^{ex3op/ex3op}$ mice also displayed increased engraftment of donor cells within the myeloid, B cell, and T cell lineages through 20 weeks compared with recipient mice transplanted with BM cells from *Kras*$^{nat/nat}$ mice (**Figure 10**).

In order to assess for LT-HSC content in *Kras*$^{ex3op/ex3op}$ mice, we performed secondary competitive repopulation assays using 1×10^6 BM cells collected from primary recipient mice at 20 weeks after transplant, along with 2×10^5 competitor BM cells. Secondary recipient mice transplanted with BM cells from primary recipient mice in the *Kras*$^{ex3op/ex3op}$ mice group demonstrated significantly decreased donor hematopoietic cell engraftment at 16 weeks after transplant compared with mice transplanted with control BM cells (**Figure 10**). This exhaustion of hematopoietic repopulating capacity was most evident within $CD11b^+$ myeloid cells, $CD3^+$ T cells, and in the BM KSL population in secondary recipients. These results suggest that a small increase in KRAS protein levels caused the expansion of HSCs with short-term repopulating capacity but resulted in the exhaustion of LT-HSCs.

Kras$^{ex3op/ex3op}$ mice display augmented hematopoietic regeneration following myelosuppression

Since BM HSCs in *Kras*$^{ex3op/ex3op}$ mice displayed increased colony-forming capacity and competitive repopulating capacity in primary recipient mice, we hypothesized that *Kras*$^{ex3op/ex3op}$ mice would have augmented hematopoietic regenerative capacity following myelosuppression. We therefore irradiated *Kras*$^{ex3op/ex3op}$ mice and *Kras*$^{nat/nat}$ mice with 750 cGy total body

irradiation (TBI), which causes severe myelosuppression, and evaluated hematopoietic recovery in both groups. At day +14, *Kras*$^{ex3op/ex3op}$ mice displayed accelerated recovery of PB WBCs, neutrophils, and lymphocytes compared with control mice (**Figure 11**). We observed no difference in BM cell counts or in percentages or numbers of BM KSL cells or ckit^{+}sca1^{-}lin^{-} myeloid progenitors between *Kras*$^{ex3op/ex3op}$ mice and *Kras*$^{nat/nat}$ mice at day +14 following irradiation (**Figure 11**). However, *Kras*$^{ex3op/ex3op}$ mice contained significantly increased BM CFCs at day +14 compared with *Kras*$^{nat/nat}$ mice (**Figure 11**). The accelerated recovery of myelopoiesis and mature neutrophils in *Kras*$^{ex3op/ex3op}$ mice was also associated with a significant improvement in survival following TBI (**Figure 11**). Eight of 17 *Kras*$^{ex3op/ex3op}$ mice (46%) remained alive at day +30 following 750 cGy TBI, compared with 2 of 17 of the *Kras*$^{nat/nat}$ mice (14%, $P = 0.03$).

Whole transcriptome analysis of HSCs in *Kras*$^{ex3op/ex3op}$ suggest augmented proliferation

We analyzed the whole transcriptome of HSCs *Kras*$^{ex3op/ex3op}$ compared to *Kras*$^{nat/nat}$ using RNA sequencing (RNA-seq). The top pathway changes were cell cycle, inflammatory response, cancer, DNA replication, and nucleic acid metabolism (**Figure 12**). Upstream analysis predicted that along with RAS proteins and ERK1/2, E2F was an important regulator. Given that, we next assessed the proliferative phenotype in relation to cell cycle regulators downstream of KRAS.

HSCs in *Kras*$^{ex3op/ex3op}$ mice demonstrate an increase in Cdk4/6–dependent repopulating capacity

RAS proteins transduce information from the cell surface that regulates numerous cellular mechanisms, including proliferation, differentiation, and survival[1,15,16,37,41-43]. Since *Kras*$^{ex3op/ex3op}$ mice displayed expansion of phenotypic and functional HSCs and progenitor cells, we compared the baseline proliferation status and survival of HSCs in *Kras*$^{ex3op/ex3op}$ mice versus *Kras*$^{nat/nat}$ mice. Twenty-four hours following administration of BrdU, *Kras*$^{ex3op/ex3op}$ mice demonstrated significantly increased proliferation of BM KSL cells, ckit^{+}sca1^{-}lin^{-} myeloid progenitors, CD11b/Gr1^{+} myeloid cells, and CD3^{+} T cells, but no difference in proliferation of CLPs or B220^{+} B cells compared with control mice (**Figure 13**). After continuous BrdU administration, we also observed substantially increased BrdU incorporation in BM HSCs at day +5 and day +25 in *Kras*$^{ex3op/ex3op}$ mice (**Figure 13**). We observed no differences in annexin^{+}7AAD^{+} cells or annexin^{+}7AAD^{-} cells within BM HSCs, BM KSL cells, or B cells between *Kras*$^{ex3op/ex3op}$ mice and *Kras*$^{nat/nat}$ mice at baseline, suggesting no effect of increased KRAS protein levels on the survival of HSCs, progenitor cells, or B cells (**Figure 14**). We also detected no difference in the homing capacity of BM cells from *Kras*$^{ex3op/ex3op}$ mice compared with *Kras*$^{nat/nat}$ mice as an explanation for the increased in vivo repopulating capacity (**Figure 14**).

Consistent with increased stimulation of the Ras pathway, BM KSL cells from *Kras*$^{ex3op/ex3op}$ mice displayed elevated phospho-ERK1/2 (p-ERK1/2) levels in response to thrombopoietin (TPO) alone or the combination of TPO/SCF/FLT-3 ligand compared with KSL cells from *Kras*$^{nat/nat}$ mice (**Figure 13**). We note here that no differences were observed in p-AKT, p-STAT5, or p-S6 levels in BM KSL cells from *Kras*$^{ex3op/ex3op}$ mice versus *Kras*$^{nat/nat}$ mice in response to TPO

(**Figure 13**). We also found no alterations in the expression of *Cdkn2d* and *Cdkn1b*, which encode the cell cycle inhibitors, p19 and p27, respectively, in BM KSL cells from *Kras*$^{ex3op/ex3op}$ mice, but expression of *Cdkn1a*, which encodes the cell cycle inhibitor, p21, was significantly decreased (**Figure 13**)[44-46]. Treatment of BM KSL cells from *Kras*$^{ex3op/ex3op}$ mice with the ERK1/2 inhibitor, BVD-523, abrogated the expansion of BM hematopoietic progenitor cells observed in *Kras*$^{ex3op/ex3op}$ mice, suggesting that the amplification of the hematopoietic compartment in *Kras*$^{ex3op/ex3op}$ mice was mediated through ERK1/2 (**Figure 15).** We hypothesized further that ERK1/2–mediated suppression of p21 might be contributing to HSC proliferation in *Kras*$^{ex3op/ex3op}$ mice by relieving p21-mediated inhibition of cyclin-dependent kinases. Indeed, BM KSL cells from *Kras*$^{ex3op/ex3op}$ mice displayed significantly increased levels of phosphorylated retinoblastoma tumor suppressor protein (p-Rb), consistent with inactivation of Rb by either Cdk4/cyclin D or Cdk2/cyclin E (**Figure 15**)[47,48]. Further, we observed increased expression of E2F-regulated cell cycle regulatory genes, including CCNE1, B-MYB, and CDK1, in BM KSL cells in *Kras*$^{ex3op/ex3op}$ mice, in keeping with Rb inactivation (**Figure 15**)[49-51]. Importantly, treatment of BM KSL cells from *Kras*$^{ex3op/ex3op}$ mice with the CDK4/6 inhibitor, palbociclib, suppressed the amplification of BM hematopoietic progenitors, suggesting that the increased HSC proliferative capacity was dependent on ERK1/2–mediated augmentation of CDK4/6 activation (**Figure 15**).

In order to determine if the enhanced in vivo repopulating capacity of HSCs in *Kras*$^{ex3op/ex3op}$ mice was also dependent on CDK4/6 activation, we performed BM transplantation of 1×10^5 BM cells

from *Kras*$^{ex3op/ex3op}$ mice versus *Kras*$^{nat/nat}$ mice into syngeneic recipient mice and then treated recipient mice with or without palbociclib. Mice transplanted with a limiting dose of BM cells from *Kras*$^{ex3op/ex3op}$ mice displayed increased survival compared with recipients of the identical dose of BM cells from control *Kras*$^{nat/nat}$ mice (**Figure 15**). However, treatment with palbociclib abrogated the augmented in vivo repopulating capacity of BM cells from *Kras*$^{ex3op/ex3op}$ mice, yielding significantly decreased survival (**Figure 15**). At day +14, mice transplanted with BM cells from *Kras*$^{ex3op/ex3op}$ mice displayed accelerated recovery of BM cell counts and KSL stem/progenitor cells compared with mice transplanted with BM from *Kras*$^{nat/nat}$ mice, while treatment with palbociclib suppressed this augmented hematopoietic recovery in recipients of *Kras*$^{ex3op/ex3op}$ BM cells (**Figure 15**). These results suggested that the augmented regenerative capacity of hematopoietic stem/progenitor cells in *Kras*$^{ex3op/ex3op}$ mice was dependent on CDK4/6 activation.

Kras regulates hematopoiesis in a cell-autonomous manner

In order to determine if the hematopoietic effects observed in *Kras*$^{ex3op/ex3op}$ mice were cell autonomous in nature, we transplanted wild-type (*Kras*$^{nat/nat}$) BM cells into irradiated *Kras*$^{ex3op/ex3op}$ mice to generate chimeric *nat;ex3op* mice. In order to control for the TBI and transplantation effects, we compared the hematopoietic phenotype of *nat;ex3op* mice with that of control mice transplanted with *Kras*$^{nat/nat}$ BM cells (nat;nat mice, controls). At 8 weeks after transplant, all mice in both groups demonstrated high donor chimerism (range 91%–98%) in the PB. Analysis of the PB of *nat;ex3op* mice revealed no increases in PB WBCs, lymphocytes, or B

cells compared with control mice and no differences in BM cell counts, KSL cells, or HSCs between *nat;ex3op* mice and control mice (**Figure 16**). A small increase in PB neutrophils was noted in *nat;ex3op* mice compared with control mice. These results suggested that the amplification of HSCs, progenitor cells, and B cells observed in $Kras^{ex3op/ex3op}$ mice was caused by hematopoietic cell–autonomous effects of increased wild-type *Kras*, rather than indirect effects via the BM microenvironment.

Chapter 3

Discussion

Activating an oncogenic version of the endogenous *Kras* gene in the hematopoietic system results in a fatal myeloproliferative disease characterized by hypersensitivity to growth factors and hyperproliferation[16], suggesting that KRAS plays a critical role in normal hematopoiesis. In order to directly test this hypothesis, we took advantage of a novel approach to studying signaling biology, namely producing more protein through silent mutations that change codon usage without altering any other feature of the gene. Using this approach, we demonstrate that increasing wild-type KRAS protein levels in BM HSCs of $Kras^{ex3op/ex3op}$ mice promotes the proliferation and expansion of HSCs capable of primary competitive repopulation and increased hematopoietic regeneration following irradiation, without any evidence of myeloproliferative disease or leukemia.

We show that wild-type KRAS activates dormant HSCs while low levels of KRAS are important for maintaining stem cell quiescence to avert exhaustion. We also present evidence that overexpression of wild-type KRAS, which retains responsiveness to GTPase-activating proteins (GAPs), has outcomes distinct from the GAP-insensitive oncogenic form. Our results indicate increasing the wild-type KRAS level is not sufficient to initiate leukemia but is sufficient to promote hematopoietic progenitor self-renewal while preserving differentiation, though with a long-term detriment to HSCs. This is consistent with other work showing that activation of HSCs during inflammation reduces competitive fitness with sustained Toll-like receptor signaling[52] or via successive divisions from aging[53]. While wild-type mice have a quiescent population of label-retaining HSCs that divide only once every 145 days on average[53,54], virtually all of the ex3op HSCs have undergone division after only 25 days. The robust induction of HSC proliferation was able to restore bone marrow function more quickly, resulting in enhanced animal survival

following a lethal dose of radiation. However, the long-term effect was HSC exhaustion in secondary CRU recipients.

Admittedly, while no mutations in *Ras* genes were detected, we cannot rule out that the higher levels of wild-type KRAS did not promote the expansion of HSCs with other mutations, and it remains to be determined whether such an increase could predispose other oncogenic mutations to be more leukemogenic. However, the highly penetrant phenotype and normal appearance of the BM suggests that the increased regenerative capacity of HSCs was a feature of elevated KRAS protein expression. Interestingly, elevated KRAS ultimately led to exhaustion of LT-HSCs in secondary transplantation assays, indicating that this proliferative effect has an upper limit. We contrast our observation with prior studies using *Mx1-Cre;Nras*$^{G12D/+}$ mice, which showed that expression of a single allele of the *Nras-G12D* oncogene in the hematopoietic compartment increased LT-HSC function as measured by serial transplantation assays[20]. While we did not perform limiting-dilution assays to estimate HSC frequency in this study, our competitive secondary transplant assays suggested a loss of LT-HSCs in *Kras*$^{ex3op/ex3op}$ mice. The divergent effects of wild-type *Kras* expression and *Nras-G12D* expression on LT-HSC function may be related to fundamental differences in KRAS and NRAS cellular activities[55,56] or sustained *Nras* oncogene expression versus wild-type *Kras* expression. In this regard, Ras dosage has been shown to promote unique effects on hematopoietic cells and the observed loss of LT-HSC repopulating capacity in *Kras*$^{ex3op/ex3op}$ mice may be a function of modest Ras dosage relative to Ras oncogene models[19,22].

Kras$^{ex3op/ex3op}$ mice also displayed PB lymphocytosis, which was caused by increased CD19^{+} B cells in the absence of alterations in T cell populations. This observation contrasts with the described effects of oncogenic *Kras-G12D* expression in the hematopoietic compartment, which produced a rapidly fatal myeloproliferative disease in mice[16,18,21]. However, conditional deletion of *Kras* in the hematopoietic compartment in mice was associated with decreased B cell numbers, in addition to increased neutrophil counts and splenomegaly[31]. This result, coupled with our findings, suggest that wild-type KRAS has a physiologic role in regulating B cell content.

We show that elevated levels of wild-type KRAS augment the hematopoietic colony–forming capacity of HSCs, which is dependent on ERK1/2 activation. In the activated state, ERK1/2 translocates to the nucleus and regulates the activity of several transcription factors, including c-Jun, c-Myc, and c-Fos, which in turn induce or repress the expression of regulatory genes[57,58]. ERK1/2 activation has been shown to be required for cellular induction of p21 expression in response to mitogens[57,59]. Interestingly, we observed decreased p21 expression in BM KSL cells in *Kras*$^{ex3op/ex3op}$ mice in association with increased ERK1/2 phosphorylation. This could be explained by ERK1/2–mediated activation of c-Myc or c-Jun, which can repress transcription of p21[57-59]. p21 abrogates cell cycle progression via inhibition of CDKs, including CDK2, CDK4, and CDK6 ([44]). Here, we demonstrated that administration of the CDK4/6 inhibitor, palbociclib, repressed both in vitro hematopoietic colony formation and in vivo repopulating capacity of BM HSCs from *Kras*$^{ex3op/ex3op}$ mice, suggesting that KRAS-mediated augmentation of HSC functional activity occurred via activation of CDK4/6. The increased levels of p-Rb in BM KSL cells from *Kras*$^{ex3op/ex3op}$ mice further support this hypothesis.

Consistent with our model, enforced expression of CDK4 in human HSCs was previously shown to promote G_0 to G_1 transit and improved HSC repopulating capacity in NOD/SCID IL-2 receptor γ chain–deficient (NSG) mice[60]. CDK6 has also been shown to regulate the timing of murine HSC exit from quiescence while conferring a competitive repopulation advantage[61]; while long-term HSCs contain almost no CDK6, short-term HSCs contain high CDK6 protein levels that permit rapid cell cycle entry upon mitogenic stimulation.

Furthermore, CDK4/6 inhibition was shown to protect HSCs from chemotherapy-induced exhaustion, in keeping with our observation that increased KRAS signaling produced CDK4/6 activation, yielding exhaustion of LT-HSCs in *Kras*$^{ex3op/ex3op}$ mice[62]. Finally, our observation of HSC exhaustion in the *Kras*$^{ex3op/ex3op}$ mice in association with decreased p21 expression is consistent with prior studies showing that p21 deficiency increased HSC proliferation and number but decreased HSC serial repopulating capacity[63].

Nonetheless, given the survival benefit demonstrated in *Kras*$^{ex3op/ex3op}$ mice following lethal dose TBI and in recipient mice following transplantation of BM cells from *Kras*$^{ex3op/ex3op}$ mice, short-term pharmacologic activation of KRAS signaling may have therapeutic potential as a strategy to promote hematopoietic regeneration following myelosuppression. In order to clarify the potential therapeutic benefit of KRAS activation, future studies will pursue characterization of the hematologic profiles of *Kras*$^{ex3op/ex3op}$ mice over time following sublethal irradiation and chemotherapy. In principle, a pharmacologic strategy to temporarily induce KRAS signaling could

harness the beneficial effects of KRAS activation in HSCs while avoiding the exhaustion of HSCs that we have observed in mice with unrelieved KRAS signal.

Since KRAS activation can affect cells within the BM microenvironment[64], we also sought to determine whether the hematopoietic phenotype of *Kras*$^{ex3op/ex3op}$ mice was caused by hematopoietic cell–autonomous effects or via indirect effects through the BM niche. Interestingly, 8-week-old chimeric *nat;ex3op* mice displayed no expansion of BM HSCs, KSL progenitor cells, or B cells as was observed in *Kras*$^{ex3op/ex3op}$ mice. This suggests that these effects of increased KRAS protein on hematopoiesis occurred in a hematopoietic cell–autonomous manner, independent from any effects on the BM microenvironment. Of note, *nat;ex3op* mice displayed an increase in PB neutrophils compared with *nat;nat* control mice, suggesting the possibility that the *Kras ex3op* allele in the BM niche may alter myeloid cell production or differentiation in vivo. This will be the subject of future studies.

Finally, our results suggest the intriguing possibility that natural variation in KRAS expression in the human population may contribute to observed variability in the regenerative potential of hematopoietic grafts from human BM or PB stem cell donors. Insufficient PB stem cell collection occurs in up to 15% of autologous donors and graft failure occurs in 5 – 15% of adult transplant recipients of cord blood and from older BM donors[65-68]. It would be of interest to determine if alterations in KRAS protein expression correlate with variations in human hematopoietic graft function. More broadly, this study provides principal demonstration of codon usage in a mammal

having a biological consequence, which may speak to the importance of codon usage in mammalian biology.

Chapter 4

Figures

Figure 1

Amino Acid	R	E	Q	I	K	R	V	K	D	S	E	D	V	P	M	V	L	V
Kras^{native}	agA	GAA	CAA	AUU	AAA	AGA	GUA	AAG	GAC	UCU	GAA	GAU	GUG	CCU	AUG	GUC	CUG	GUA
Kras^{ex3op}	agA	GAA	CAA	AUU	AAG	AGA	GUG	AAG	GAC	UCC	GAG	GAC	GUG	CCU	AUG	GUG	CUG	GUG

Amino Acid	G	N	K	C	D	L	P	S	R	T	V	D	T	K	Q	A	Q	E
Kras^{native}	GGG	AAU	AAG	UGU	GAU	UUG	CCU	UCU	AGA	ACA	GUA	GAC	ACG	AAA	CAG	GCU	CAG	GAG
Kras^{ex3op}	GGC	AAC	AAG	UGC	GAC	CUC	CCU	AGC	AGA	ACC	GUG	GAC	ACC	AAG	CAG	GCC	CAG	GAG

Amino Acid	L	A	R	S	Y	G	I	P	F	I	E	T	S	A	K	T	R	Q
Kras^{native}	UUA	GCA	AGG	AGU	UAC	GGG	AUU	CCG	UUC	AUU	GAG	ACC	UCA	GCA	AAG	ACA	AGA	CAG
Kras^{ex3op}	CUG	GCC	AGG	AGC	UAC	GGC	AUC	CCU	UUC	AUC	GAG	ACC	AGC	GCC	AAG	ACA	AGA	CAG

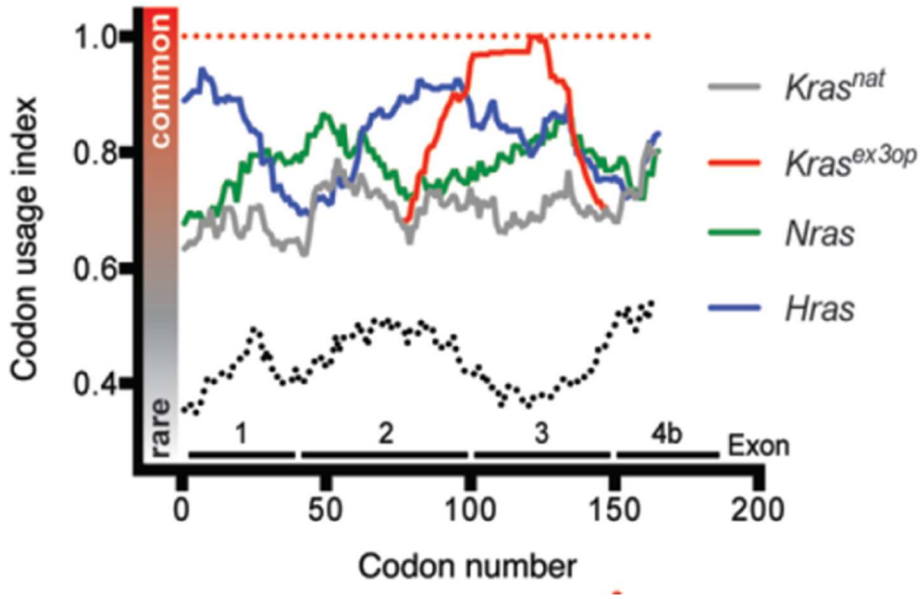

Figure 1. Kras is enriched for rare codons. (**Top**) Position of synonymous mutations (red) in *Kras*^{ex3op} aligned to *Kras*^{nat} within exon 3. Lowercase letters denote nucleotides from exon 2. (**Bottom**) Sliding window of codon usage index which shows the relative codon usage of the mouse *Ras* genes. Also included is the engineered enrichment of common codons in exon 3 of *Kras*^{ex3op} (red) relative to *Kras*^{nat} (gray). Theoretical Kras transcripts encoded by all common (red dotted line) or all rare (black dotted line) are plotted for reference. Adapted from Pershing[1] et al. 2015.

Figure 2

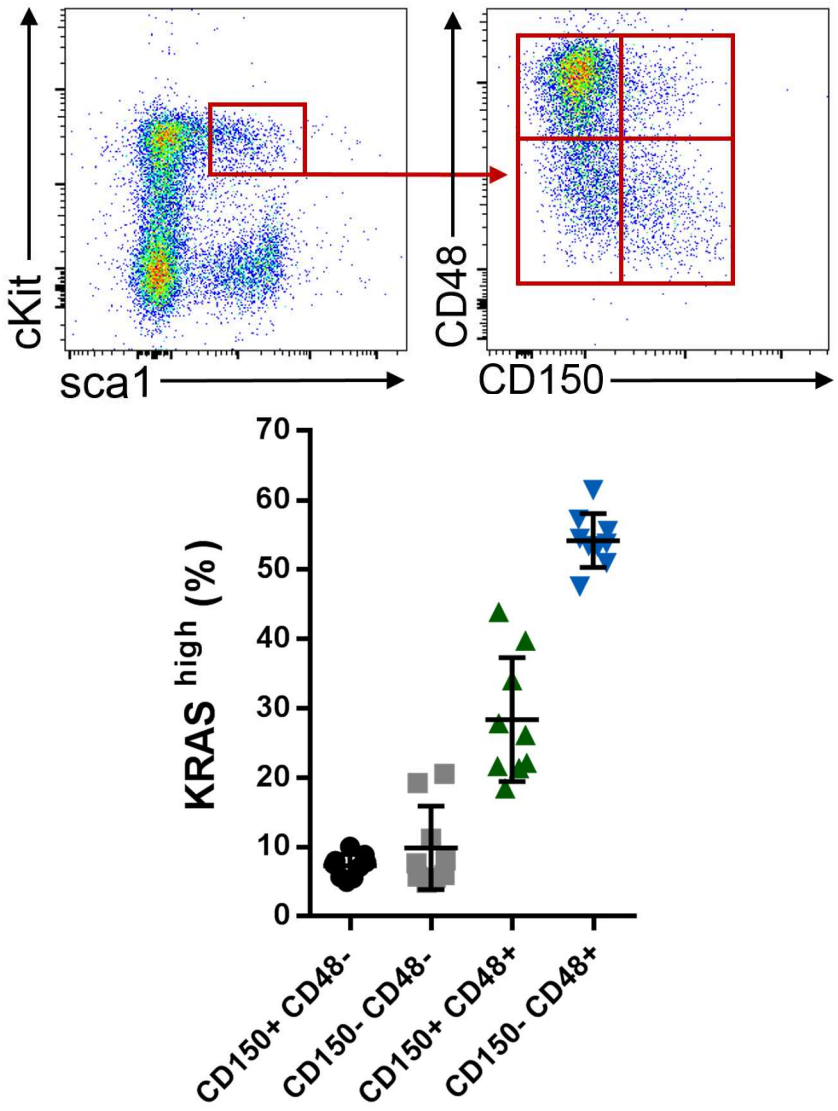

Figure 2. KRAS protein increases as HSCs differentiate into more mature progenitors. (**Top**) Representative flow cytometry plot gated on lineage negative BM cells showing KSL gate. These KSL cells are then gated according to CD150 and CD48 positivity. (**Bottom**) KRAS protein is low in HSCs but increases in progressively more mature progenitors.

Figure 3

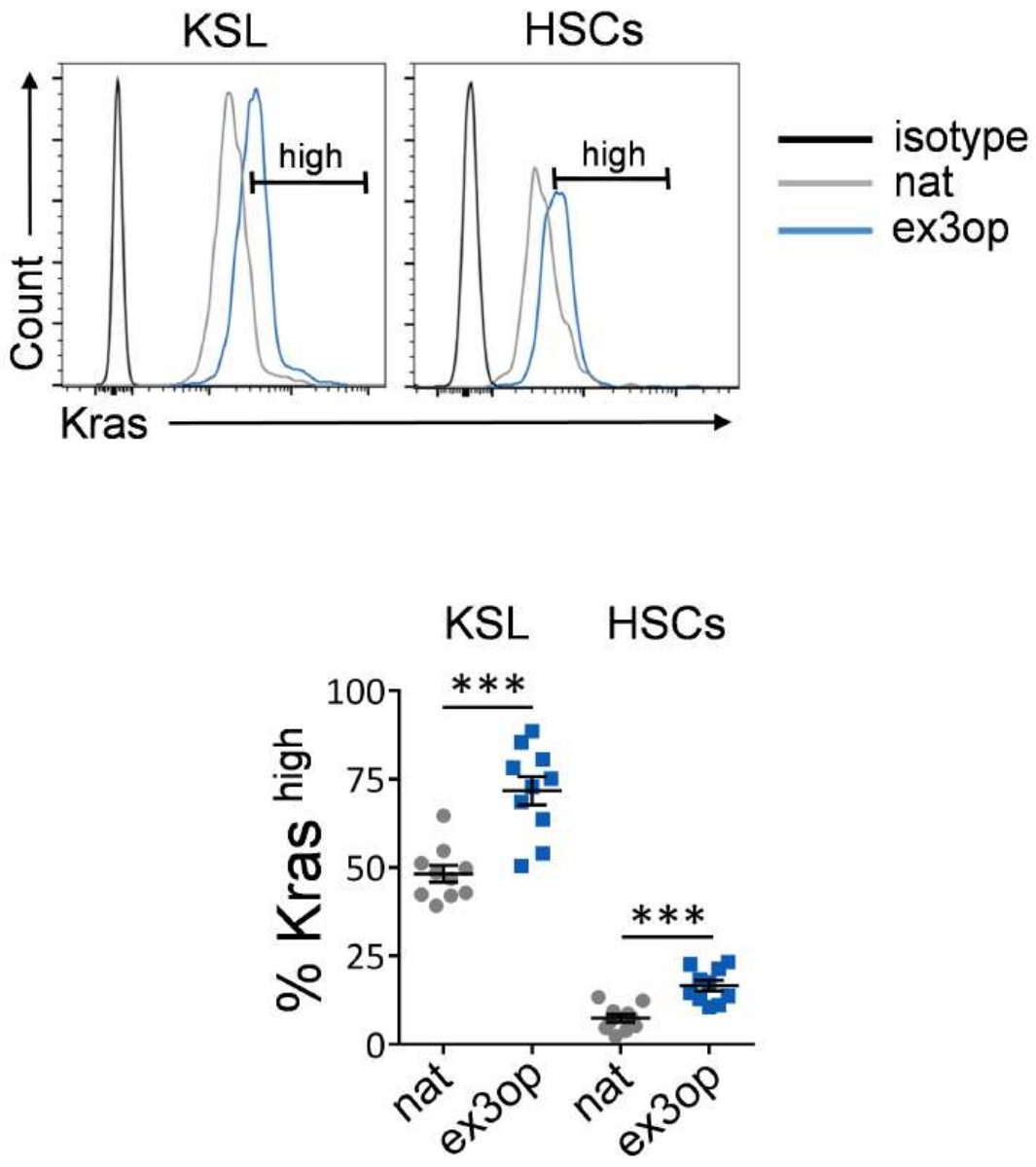

Figure 3. KRAS translation is constrained by rare codons. (Top) Representative histograms of Kras protein levels in BM KSL cells and HSCs in 8- to 12-week-old *Kras*$^{ex3op/ex3op}$ mice (ex3op) and *Kras*$^{nat/nat}$ mice (nat). Isotype control is shown in black. Gate represents KRAS ^{hi} cells. (Bottom) Mean percentages of KRAS ^{hi} cells are shown within each mouse group (n= 9/group). ***p<0.001.

Figure 4

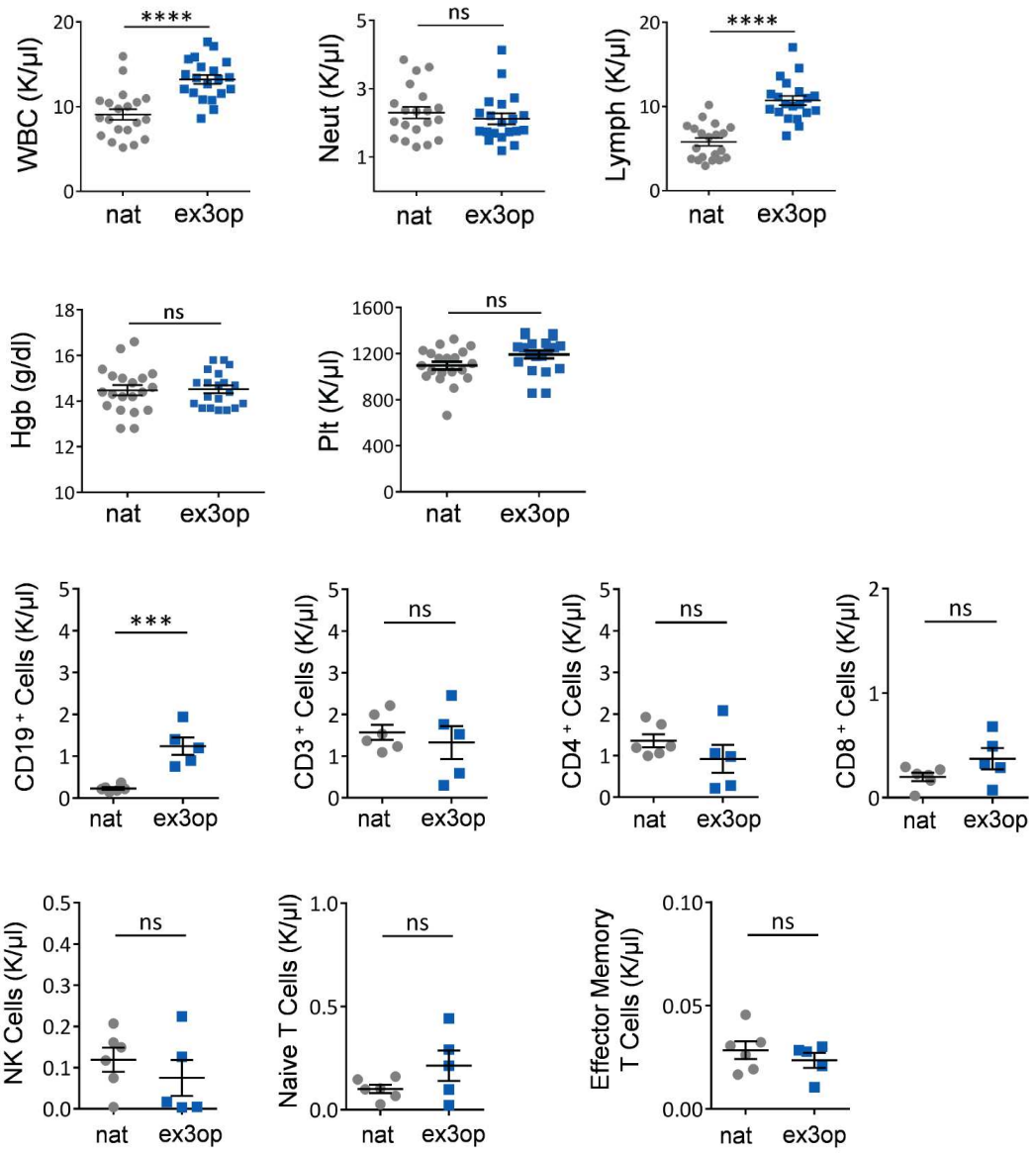

Figure 4. KRAS expands B lymphocytes. (Top two rows) Scatter plots show mean PB white blood cells (WBCs), neutrophils (Neut), and lymphocytes (Lymph) at baseline in 8- to 12-week-old *Kras*$^{ex3op/ex3op}$ mice (ex3op) and *Kras*$^{nat/nat}$ mice (nat) (n= 20/group). ****p< 0.0001. (Bottom two rows) By flow cytometry, PB CD19+ B cells, CD3+ T cells, CD4+ T cells, CD8+ T cells, NK cells, naive T cells, and effector memory T cells (n= 8/group). *** p< 0.001. Two-tailed Student's t test was used for each comparison. ns, not significant. Data are presented as mean ± SEM.

Figure 5

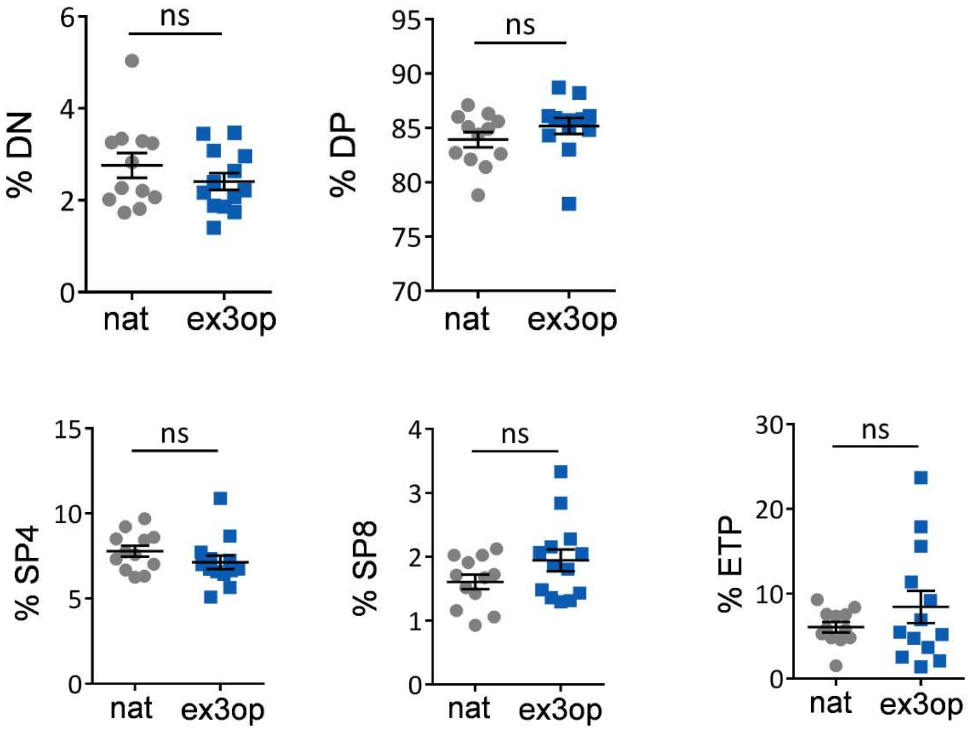

Figure 5. Thymic profile of *Kras* $^{ex3op/ex3op}$ mice. Percentages of double negative (DN) and double positive (DP) thymocytes, single positive CD4+ (SP4) and single positive CD8+ (SP8) thymocytes, and early thymic progenitor cells (ETPs) in *Kras* $^{ex3op/ex3op}$ mice (ex3op) and *Kras* $^{nat/nat}$ mice (nat).

Figure 6

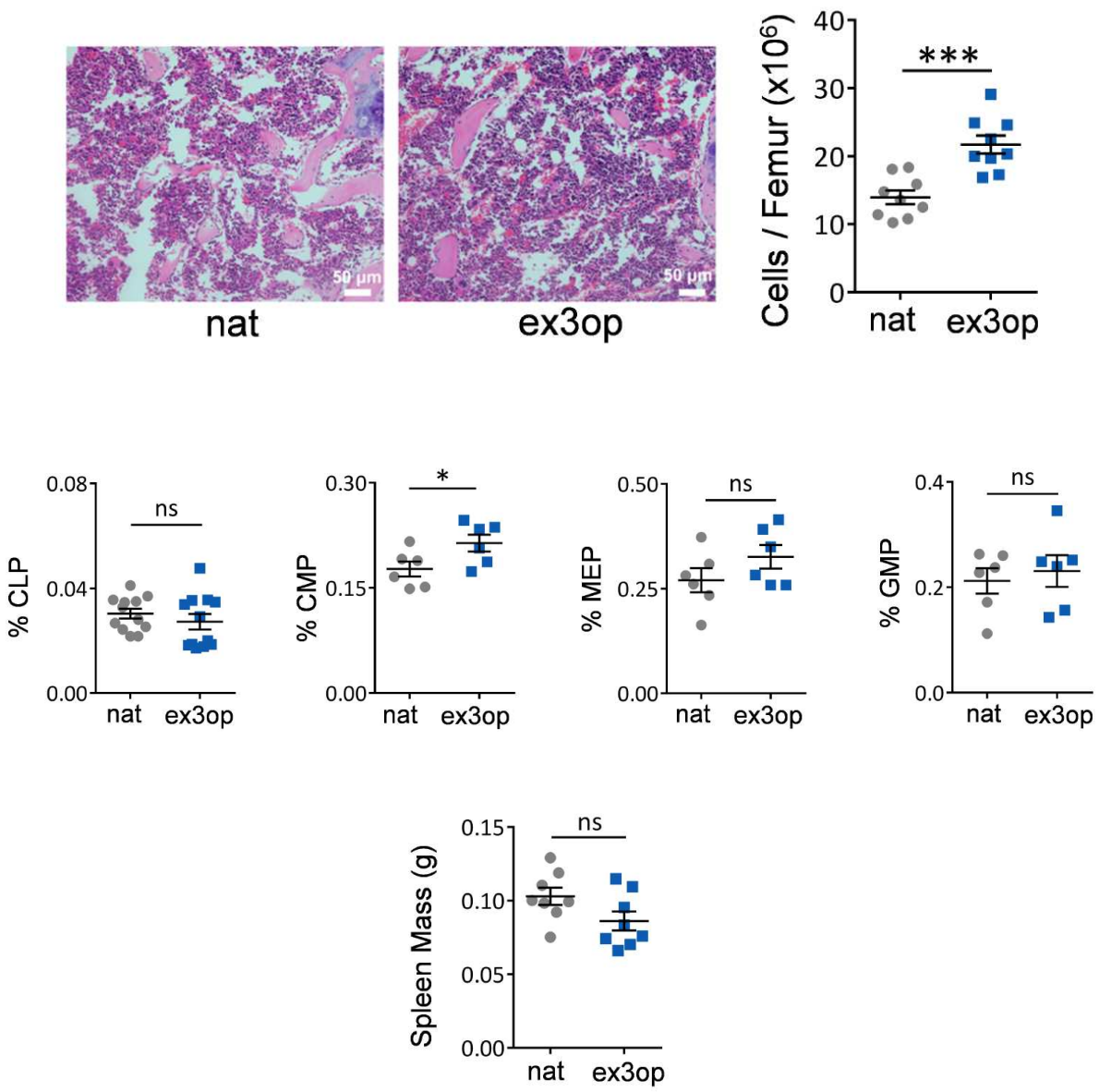

Figure 6. Bone marrow profile of *Kras* $^{ex3op/ex3op}$ mice. (**Top**) At left, representative microscopic images of femurs from *Kras* $^{ex3op/ex3op}$ mice (ex3op) and *Kras* $^{nat/nat}$ mice (nat) stained with hematoxylin and eosin;10x magnification. At right, mean numbers of BM cells/femur are shown. n=9/group, ***p<0.001. (**Middle Row**) Scatter plots show percentages of BM CLPs, CMPs, MEPs and GMPs. n=6-11/group, *p<0.05. (**Bottom**) Scatter plots show spleen masses in *Kras* $^{ex3op/ex3op}$ mice (ex3op) and *Kras* $^{nat/nat}$ mice (nat) at 8 weeks.

Figure 7

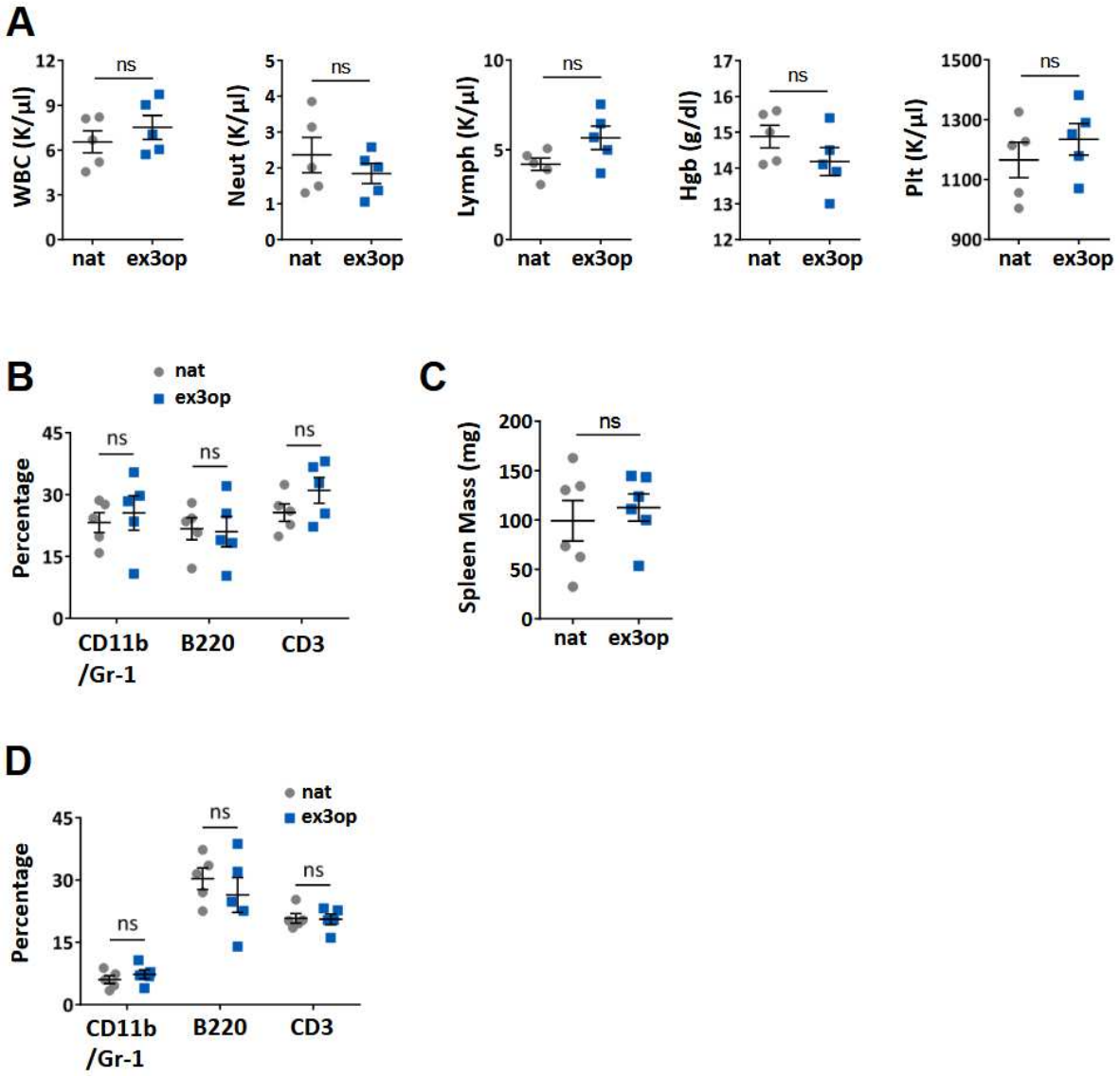

Figure 7. Twenty-month old *Kras*$^{ex3op/ex3op}$ mice show no signs of myeloproliferative disease or leukemia. (**A**) Mean PB WBCs, neutrophils, lymphocytes, hemoglobin and platelet counts in ex3op mice and nat mice at 12 months of age. n=5/group. (**B**) Scatter plots show PB myeloid cells (CD11b/Gr1), B cells (B220) and T cells (CD3) in ex3op mice and nat mice at 12 months of age. n=5/group. (**C**) Mean spleen mass in ex3op mice and nat mice at 12 months. n=6/group. (**D**) Mean percentages of myeloid cells, B cells and T cells in the spleen in 12 month old mice. n=5/group. ns = not significant. Two-tailed Student's t-test was performed for all analyses. Error bars represent means + SEM.

Figure 8

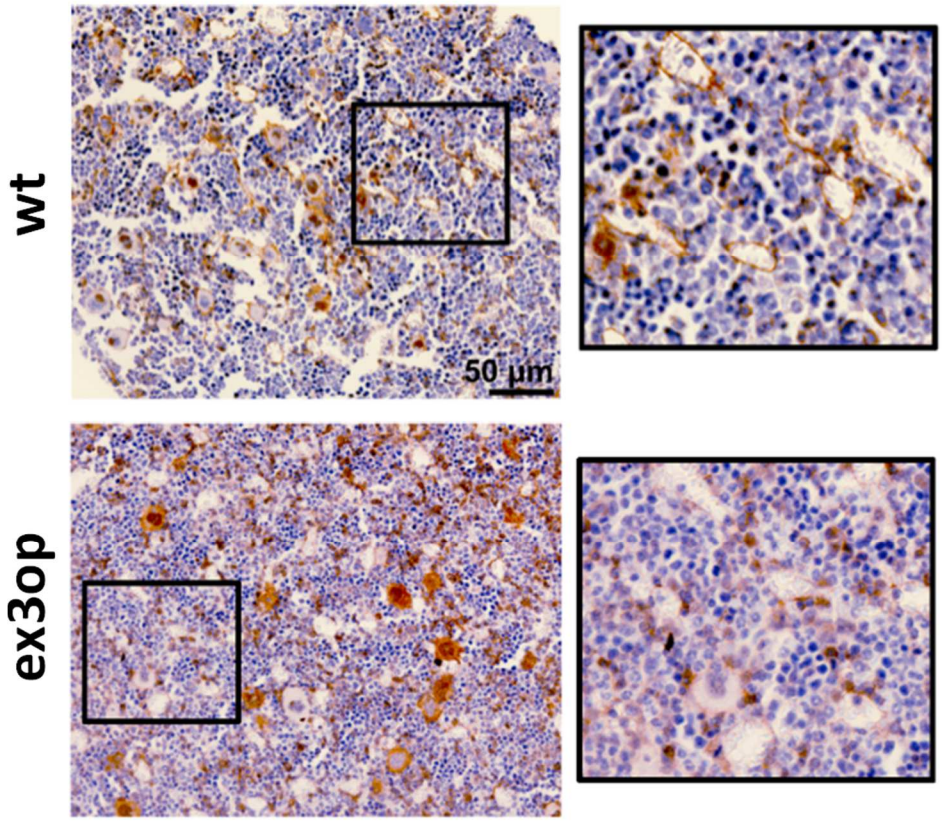

Figure 8. No major BM microenvironment change in *Kras*$^{ex3op/ex3op}$ mice. CD31 immunohistochemical stains mark endothelial cells, the predominant niche for HSCs. No expansion of the vascular niche was observed.

Figure 9

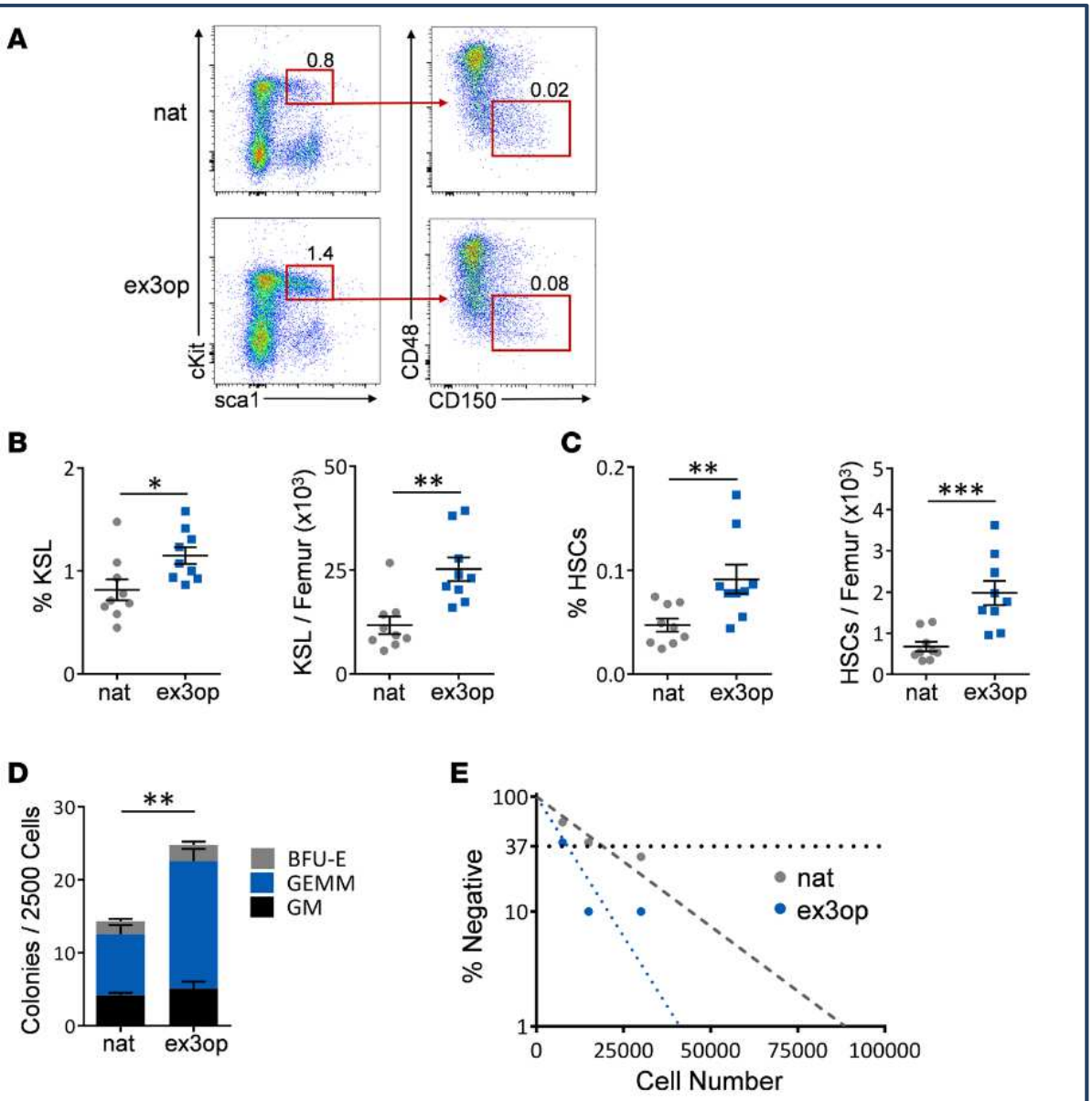

Figure 9. *Kras*$^{ex3op/ex3op}$ mice display increased BM HSCs and progenitor cells. (**A**) Representative flow cytometric analysis of BM ckit+ sca1+ lin– (KSL) cells and CD150+ CD48– KSL HSCs in ex3op mice and nat mice at baseline. Numbers represent the percentages of KSL cells and CD150+ CD48– KSL cells shown within the gates. (**B**) Mean percentages of BM KSL cells and numbers of KSL cells in ex3op mice and nat mice at baseline (n = 9/group). *p<0.05, **p<0.01. (**C**) Mean percentages of BM HSCs and numbers of HSCs in ex3op mice and nat mice (n = 9/group). **p<0.01, ***p<0.001. (**D**) Mean numbers of CFCs in ex3op mice and nat mice (n = 10/group). **p<0.01. (**E**) Poisson statistical analysis of a limiting-dilution assay revealed BM LTC-IC frequencies of 1 in 8,940 in ex3op mice and 1 in 19,235 in nat mice at 8 – 12 weeks. The plot shows the percentage of negative colonies detected at 3 different BM cell doses. The horizontal line represents the cell dose at which 37% of the plates show no colonies (n = 6/group). p= 0.03. Two-tailed Student's t test performed throughout. Data are presented as mean ± SEM.

Figure 10

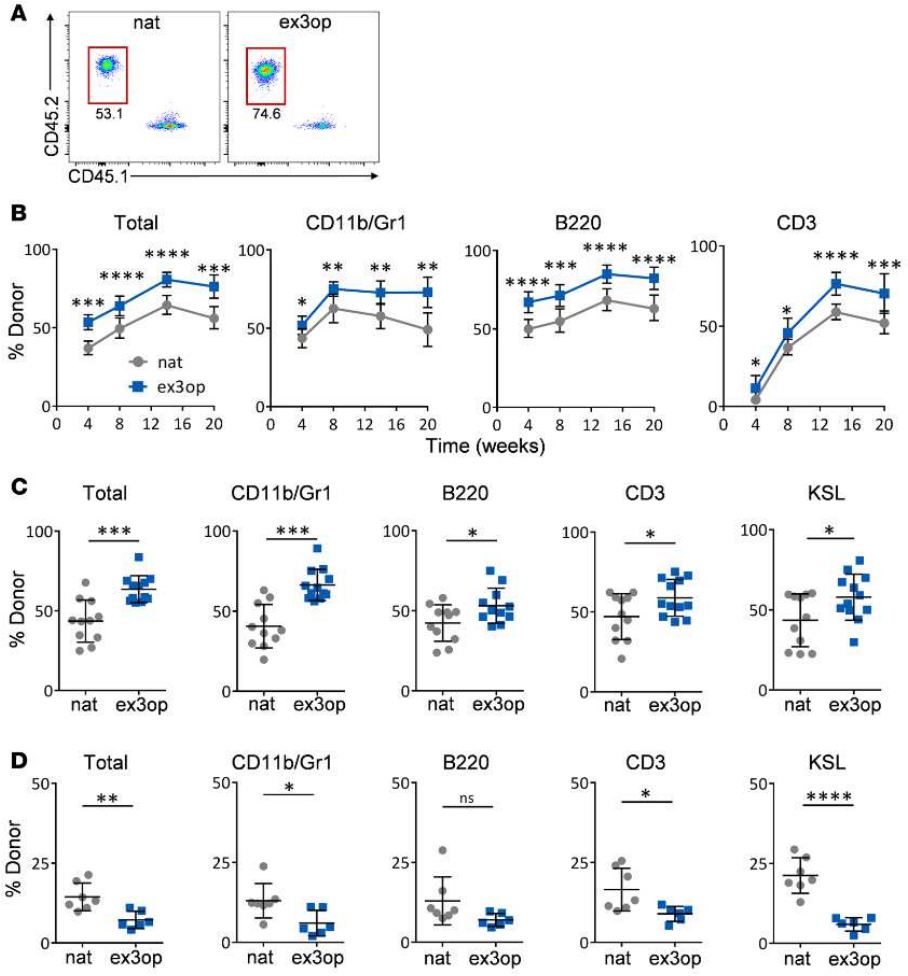

Figure 10. KRAS expands HSCs and exhausts long-term repopulating HSCs. (**A**) Representative flow cytometric analysis of donor CD45.2+ hematopoietic cell engraftment in the PB of recipient CD45.1+ mice at 20 weeks following transplantation of 2×10^5 BM cells from ex3op mice or nat mice, along with 2×10^5 competitor CD45.1+ BM cells. Numbers represent percentages in each gate. (**B**) Panels show the mean percentages (± SD) of total donor CD45.2+ cells and donor CD45.2+ cells within the CD11b+ myeloid population, B220+ B cells, and CD3+ T cells in the PB of CD45.1+ recipient mice over time following competitive transplantation of BM cells from ex3op mice (CD45.2+) or nat mice (CD45.2+) (n = 12/group). *p<0.05, **p<0.01, ***p<0.001, ****p<0.0001. (**C**) Mean percentages (± SD) of total donor CD45.2+cells and donor CD45.2+ cells within the BM CD11b+ myeloid population, B220+ B cells, CD3+ T cells, and KSL population in CD45.1+ recipient mice at 20 weeks following competitive transplantation of BM cells from ex3op mice or nat mice (n = 12/group). *p<0.05, ***p<0.001. (**D**) Panels show the percentages of donor (DsRed+) total cell engraftment, as well as donor cell engraftment within lineages of secondary recipient (DsRed-negative) mice at 16 weeks following competitive transplantation of 1×10^6 BM cells collected from primary recipient mice. Primary recipient (DsRed-negative) mice were transplanted with 2×10^5 BM cells from ex3op (DsRed-positive) mice or nat (DsRed-positive) mice, along with 2×10^5 competitor (DsRed-negative) BM cells (n = 7/group). *p<0.05, **p<0.01, ****p<0.0001. Data are presented as mean ± SD. Two-tailed Student's t test was used for all analyses.

Figure 11

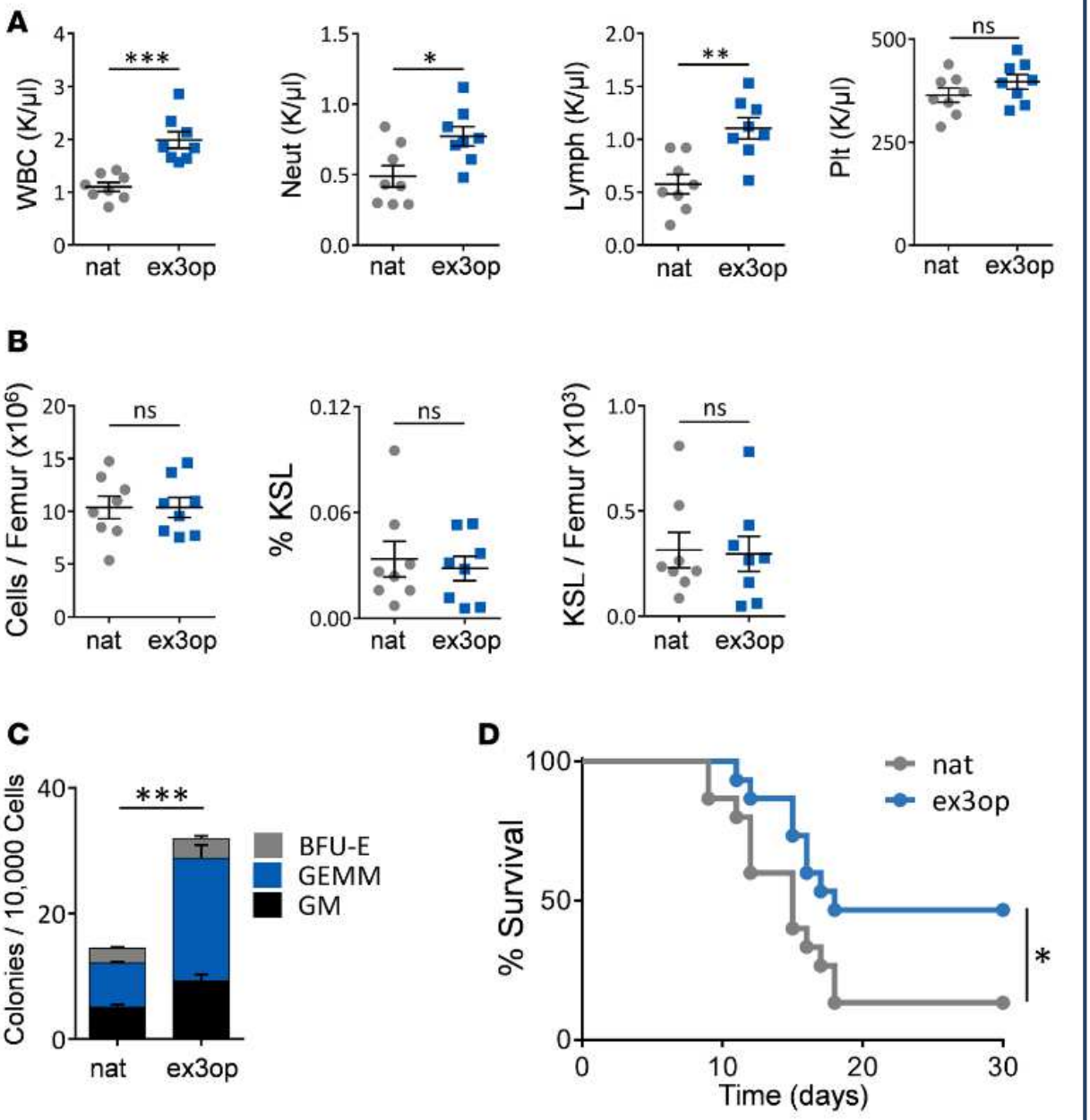

Figure 11. Increased wild-type KRAS promotes hematopoietic regeneration following myelosuppression. (**A**) Mean PB WBCs, neutrophils, lymphocytes, and platelet (Plt) counts are shown in ex3op mice and nat mice at day +14 following 750 cGy TBI (n = 10/group). *p<0.05, **p<0.01, ***p<0.001. ns, non-significant. (**B**) Mean BM cell counts, percentage of KSL cells, and numbers of KSL cells at day +14 following 750 cGy (n = 10/group). (**C**) Mean numbers of BM CFCs at day +14 (n = 10/group). ***p<0.001. (**D**) The percentage survival of ex3op mice and nat mice is shown through day +30 following 750 cGy TBI (n = 12/group). *p= 0.03 by log-rank test for survival analysis. For other analyses, Student's t tests were performed. Data are presented as mean ± SEM.

Figure 12

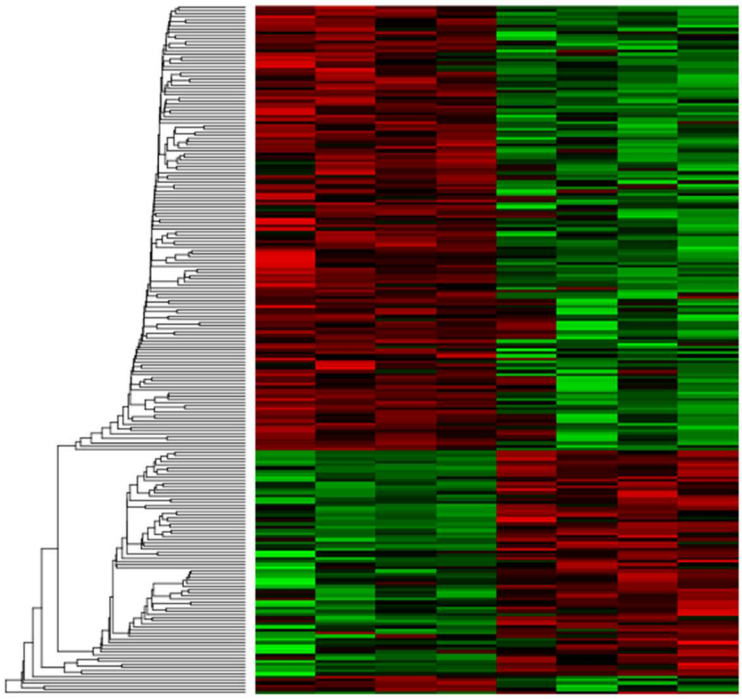

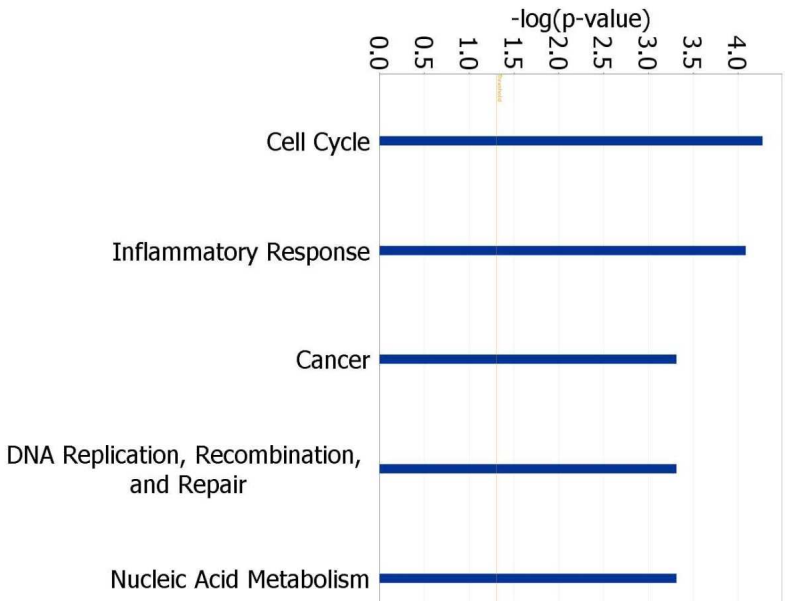

Figure 12. Transcriptome analysis of ex3op HSCs reveals activation of proliferation pathways. (**Top**) Heat map for the top differentially expressed genes in CD34 negative KSL cells (*Kras*$^{ex3op/ex3op}$ versus *Kras* $^{nat/nat}$). (**Bottom**) Top pathways activated in *Kras*$^{ex3op/ex3op}$ HSCs.

Figure 13

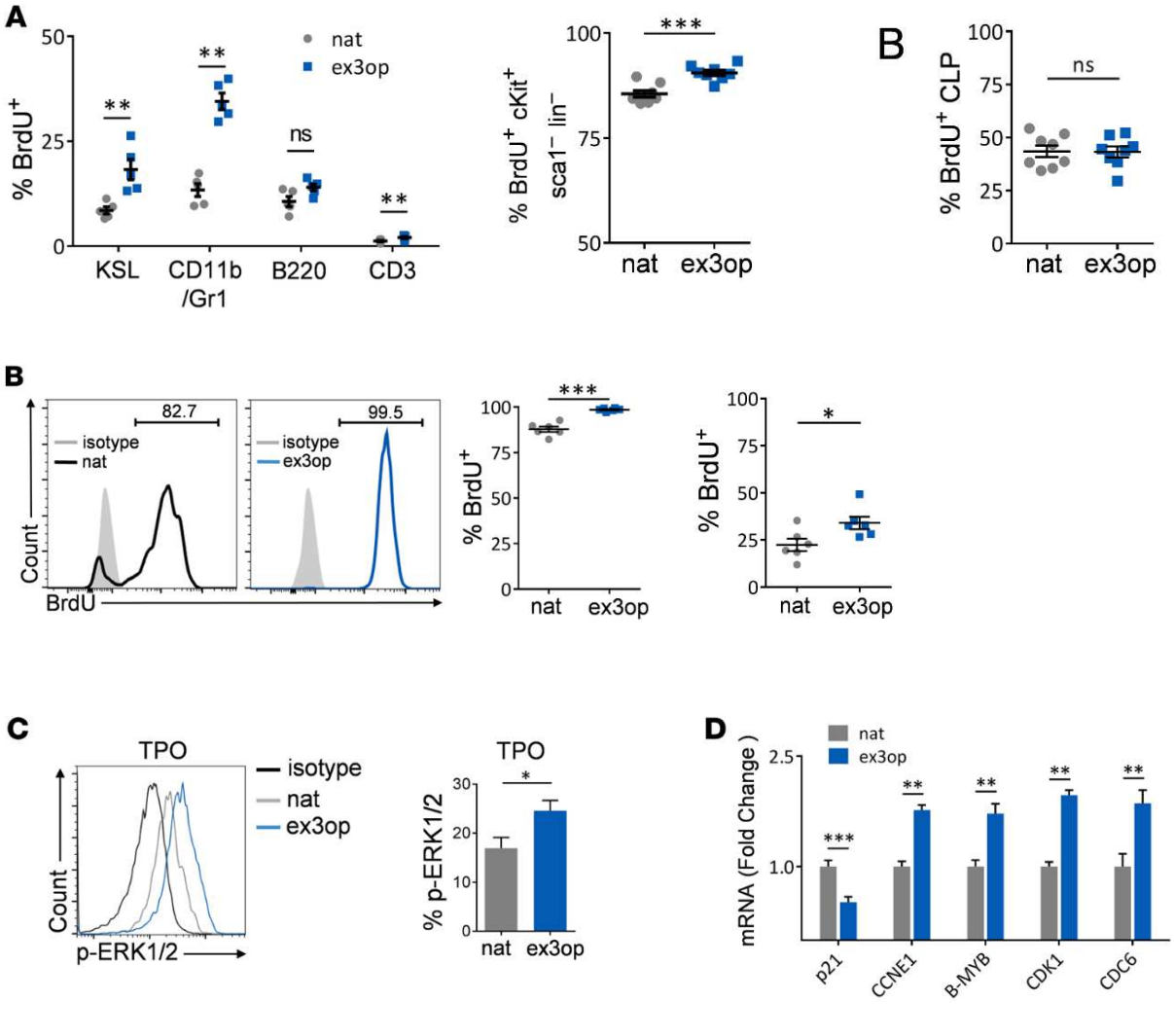

Figure 13. Wild-type KRAS augments hematopoietic repopulating capacity in a CDK4/6–dependent manner. (A) Increased percentage of ex3op BrdU-positive cells are shown within BM KSL cells, myeloid cells, B cells, T cells, and myeloid progenitor cells, but not CLPs at 24 hours after BrdU administration (n = 5-9/group). **p<0.01. (**B**) At left, representative analysis of BrdU incorporation in BM CD150+ CD48– KSL HSCs in nat mice and ex3op mice at day +25 following continuous BrdU administration in drinking water. Mean percentages of BrdU-positive HSCs at day 25 (middle) and day 5 (right) are shown in each group (n = 6/group). ***p<0.001. (**C**) At left, representative phospho-ERK1/2 (p-ERK1/2) expression in BM KSL cells from ex3op mice and nat mice in response to 20 ng/ml thrombopoietin (TPO) treatment for 5 minutes. At right, bar graphs show p-ERK1/2–positive KSL cells in each group (n = 5/group). *p<0.05. (**D**) Relative mRNA levels of cell cycle regulatory genes in BM KSL cells from ex3op mice and nat mice at baseline (n = 8/group). **p<0.01, ***p<0.001.

Figure 14

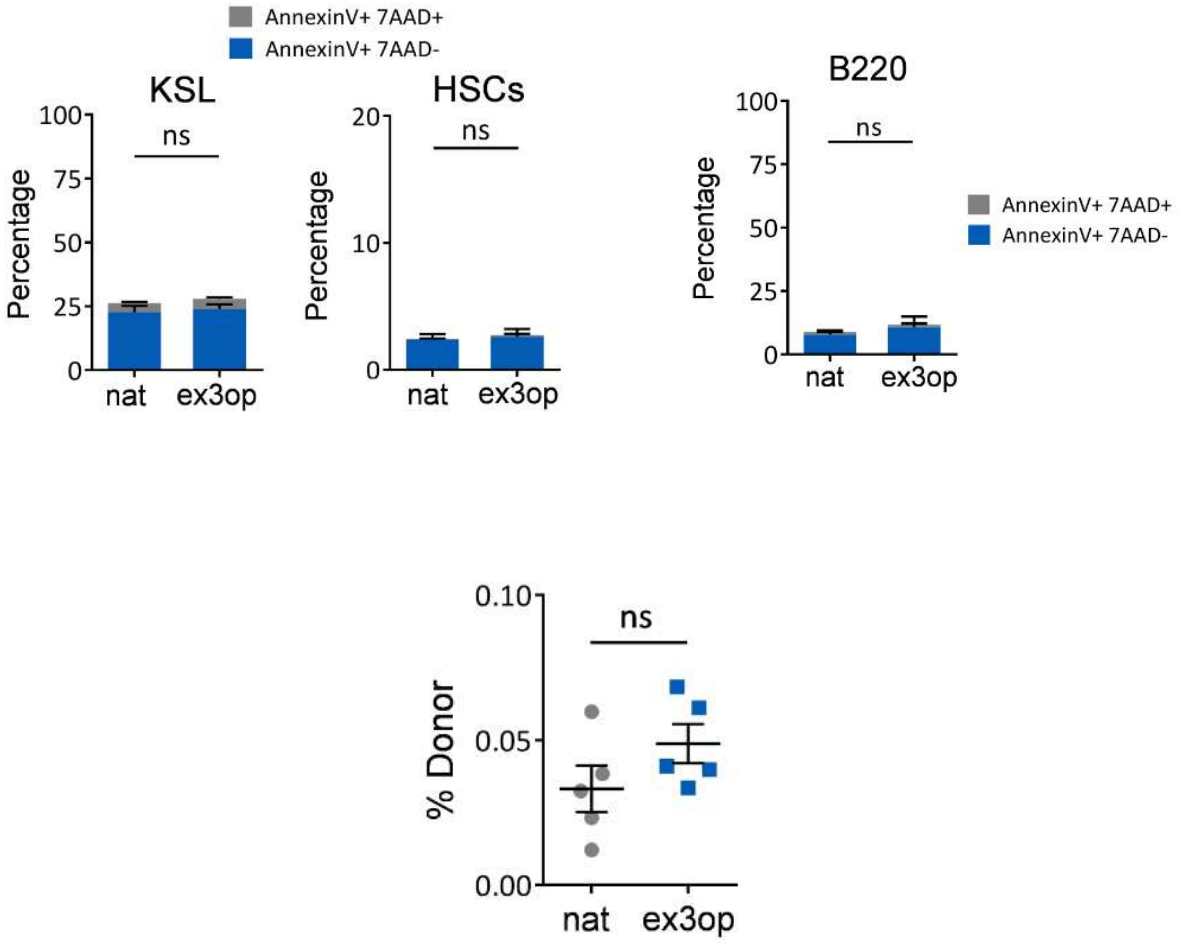

Figure 14. No change in survival or migration of *Kras* $^{ex3op/ex3op}$ cells. (**Top**) Mean percentages of Annexin+7AAD- and Annexin+7AAD+ BM KSL cells, HSCs, and B cells at baseline in 8 - 12 week-old ex3op mice and nat mice. n=6/group. (**Bottom**) Mean percentages of DsRed+ hematopoietic cells in DsRed-negative recipient mice at 18 hours following intravenous injection of $4x10^4$ BM KSL cells from *Kras*$^{ex3op/ex3op}$;DsRed+ mice or *Kras*$^{nat/nat}$;DsRed+ mice into lethally irradiated *Kras*$^{nat/nat}$ mice (DsRed-negative). n=5/group. Two-tailed Student's t-tests for all comparisons; Error bars represent means + SEM.

Figure 15

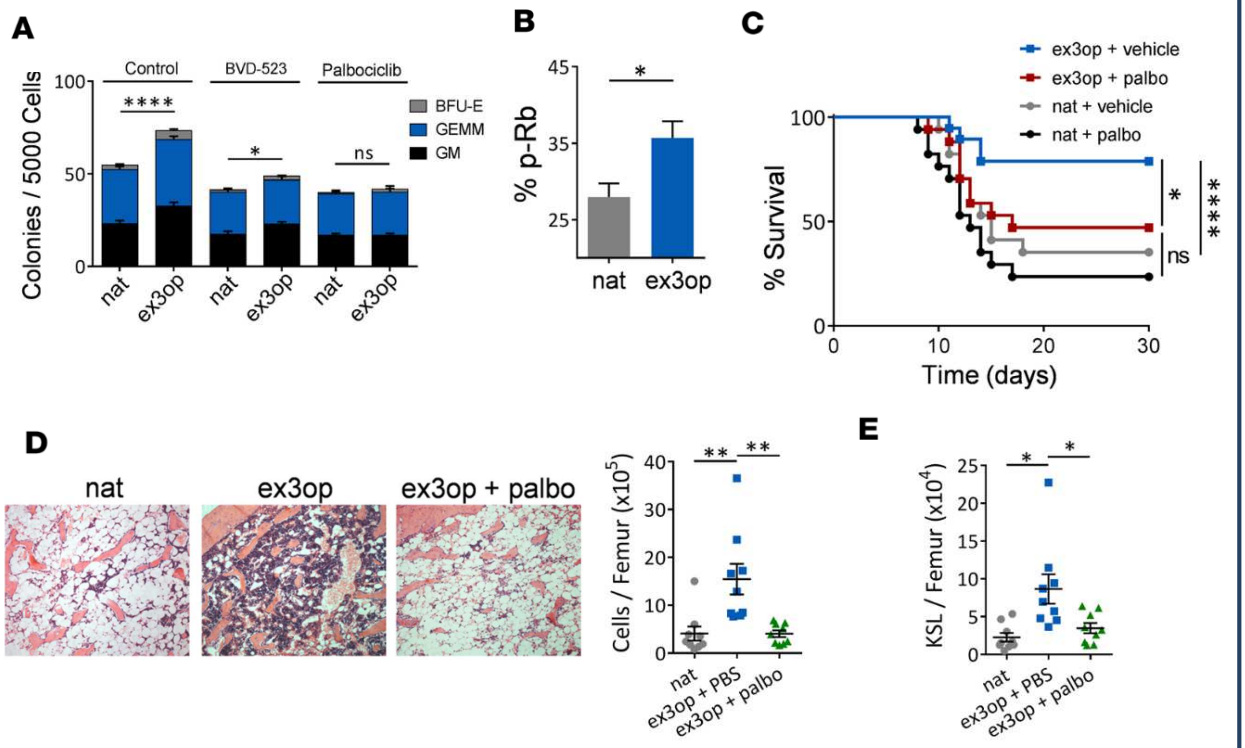

Figure 15. Wild-type KRAS augments hematopoietic repopulating capacity in a CDK4/6–dependent manner. (A) Mean numbers of CFCs following 72-hour culture of BM KSL cells from ex3op mice or nat mice with media containing TPO, stem cell factor, and FLT3 ligand (TSF), with or without the ERK1/2 inhibitor, BVD-523, or the CDK4/6 inhibitor, palbociclib (palbo) (n = 6/group). *p<0.05, ****p<0.0001. **(B)** Mean percentages of phospho-Rb (p-Rb) in BM KSL cells in ex3op mice and nat mice at baseline (n = 4/group). *p<0.05. **(C)** C57BL/6 mice were irradiated with 850 cGy TBI, and then transplanted with 1×10^5 BM cells from ex3op mice or nat mice and treated on days +5 and +6 with either 85 mg/kg palbo or saline. Percentage survival of each group of mice is shown (n = 17/group). Log-rank test was used for survival analysis. *p<0.05, ****p<0.0001. **(D)** At left, representative microscopic images of femurs stained with H&E (×10 magnification) at day +14 from irradiated mice transplanted with ex3op BM cells, nat BM cells, or ex3op BM cells + palbociclib treatment. At right, mean BM cell counts (± SEM) at day +14 are shown for each group (n = 9/group). **p<0.01. **(E)** Scatter plot shows numbers of BM KSL cells at day +14 in irradiated recipient mice transplanted with nat BM cells, ex3op BM cells, and ex3op BM cells + palbo treatment (n = 9). *p<0.05. Except as noted, p values were obtained using a 2-tailed Student's t test. Data are presented as mean ± SEM.

Figure 16

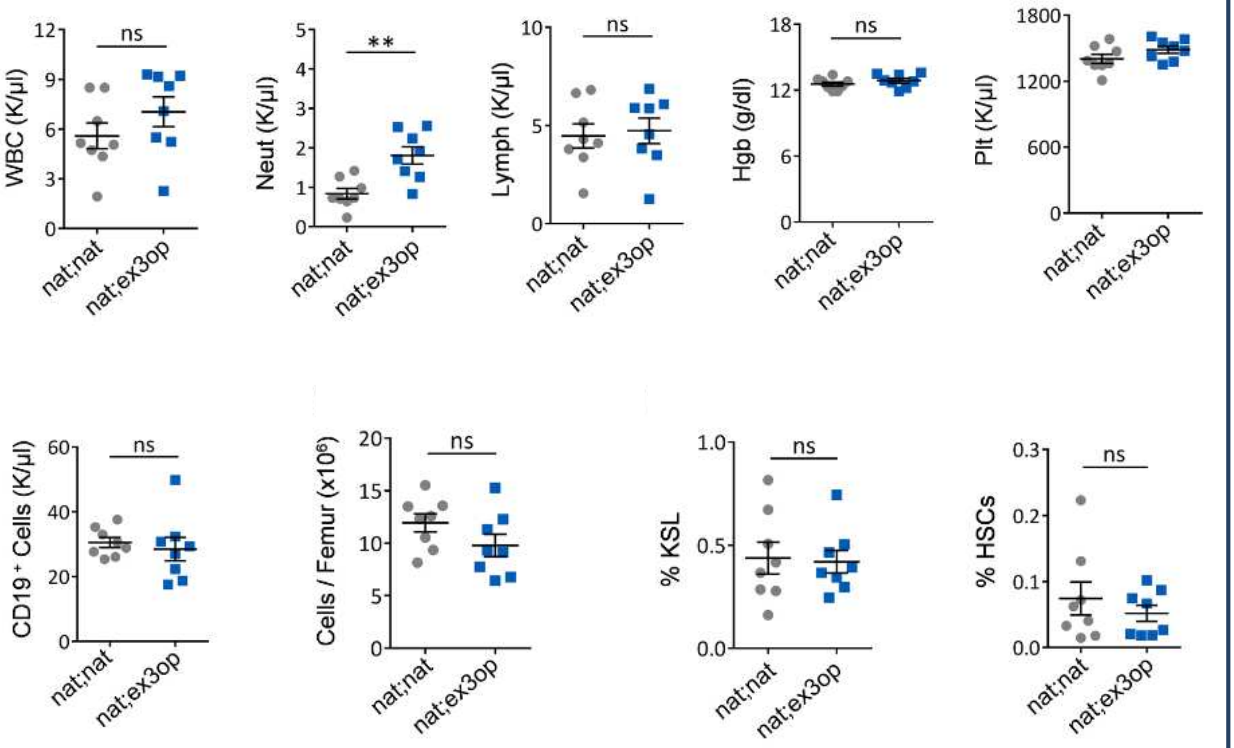

Figure 16. *Kras* regulates hematopoiesis in a hematopoietic cell–autonomous manner.
Scatter plots show no differences in PB WBCs, lymphocytes, hemoglobin (Hgb), platelets (Plt) CD19+ B cells, BM cell counts, fraction of BM KSL and HSCs between 8-week-old nat;ex3op mice and nat;nat mice. Increased PB neutrophils are detected in nat;ex3op mice (n = 8/group). **p<0.01. Data are presented as mean ± SEM. Two-tailed Student's t test was used for all analyses. ns = not significant.

Chapter 5

Materials and Methods

Mice

All animal procedures were performed in accordance with animal use protocols approved by the UCLA Animal Care and Use Committee. Generation of the *Kras*$^{ex3op/ex3op}$ mouse has been previously reported[1,36]. The *Kras*$^{ex3op/ex3op}$ mice were backcrossed 10 generations into C57BL/6 mice purchased from Jackson Laboratories (stock 000664). In some studies, *Kras*$^{ex3op/ex3op}$ mice were crossed into *β-actin-DsRed* mice (DsRed, stock 006051, Jackson Laboratories) to facilitate analysis of donor versus recipient hematopoietic cells. We measured complete blood counts using a Hemavet 950 instrument (Drew Scientific). For determination of cell-autonomous effects of *Kras*^{ex3op} mutation on hematopoiesis, we transplanted 3×10^6 BM cells from wild-type littermate control (*Kras*$^{nat/nat}$) mice into irradiated (950 cGy) *Kras*$^{ex3op/ex3op}$ mice and *Kras*$^{nat/nat}$ mice (controls). At 8 weeks of age, we confirmed greater than 90% donor CD45.1$^+$ cell chimerism in the BM of transplanted mice (*nat;ex3op* mice). We subsequently measured the PB and BM hematopoietic profiles in *nat;ex3op* chimeric mice versus *nat;nat* control mice. We used 8- to 12-week-old, age- and sex-matched mice, with wild-type littermates as controls for all mice studies, except as otherwise noted.

Competitive repopulation assays

In order to perform primary competitive repopulation assays, *Kras*$^{ex3op/ex3op}$ mice and *Kras*$^{nat/nat}$ mice were backcrossed 10 or more generations into C57BL/6 background (CD45.2$^+$) and were utilized as donor mice. Syngeneic B6.SJL (CD45.1$^+$) mice (Jackson Laboratories, stock 002014) were used as recipients. An equal dose of donor BM cells (2×10^5) and competitor BM cells ($2 \times$

10^5) was utilized for these experiments. Donor hematopoietic cell engraftment within myeloid cells, B cells, and T cells in transplanted mice was measured by flow cytometry, as previously described[20,69-72]. We also utilized *Kras*$^{ex3op/ex3op}$ mice and *Kras*$^{nat/nat}$ mice (C57BL/6 background) that were crossed into the *β-actin-DsRed* mice (C57BL/6 background) for competitive repopulation assays into lethally irradiated recipient 10-week-old female *Kras*$^{nat/nat}$ mice (DsRed-negative), following the approach described above. At 20 weeks after transplant, 1×10^6 BM cells were collected from primary recipient mice and injected via tail vein, along with 2×10^5 competitor (DsRed-negative) BM cells, into lethally irradiated secondary recipient *Kras*$^{nat/nat}$ mice (DsRed-negative). Measurement of donor hematopoietic cell engraftment within myeloid, B cell, and T cell lineages was performed as previously described [20,69-72].

Mouse cell isolation and culture

PB was collected from mice through submandibular puncture. To collect BM cells, long bones (femurs and tibia) were harvested from euthanized mice and flushed with IMDM containing 10% FBS. BM cells were filtered through a 40-μm strainer to obtain single-cell suspensions. Both PB and BM were subjected to RBC lysis using ACK RBC lysis buffer prior to FACS staining. Spleens were mechanically dissociated using a mortar and pestle and then subjected to RBC lysis. Single-cell suspensions of thymocytes were prepared by mechanical dissociation in buffer (10% FBS in PBS). We performed mouse BM lineage depletion using a mouse lineage cell depletion kit, per the manufacturer's protocol (Miltenyi Biotec). We cultured lineage-negative mouse HSCs and progenitor cells in IMDM with 10% FBS, 125 ng/ml mouse stem cell factor (SCF) (R&D Systems, 455-MC-010), 20 ng/ml mouse TPO (R&D Systems, 488-TO-005/CF), and 50 ng/ml mouse Fms-

like tyrosine kinase 3 ligand (FLT3L) (R&D Systems, 427-FL-005/CF). Where noted, palbociclib or BVD-523 was added to the media at 100 nM.

BrdU

BrdU (Sigma-Aldrich) was administered as a single dose of 150 mg per kg of body mass by intraperitoneal injection followed by 1 mg/ml BrdU in the drinking water. Analysis was performed at 24 hours. For long-term BrdU administration (5 and 25 days), BrdU water was given continuously and changed every 3 days.

Immune cell analysis and flow cytometry

Cells were analyzed by flow cytometry for myeloid ($CD11b^+/Gr\text{-}1^+$), B cell ($B220^+$), T cell ($CD3^+$), stem/progenitor cell (KSL), and HSCs as previously described[73,74]. Histograms and dot plots were created using FlowJo software (Tree Star). BrdU analysis was performed using the BrdU Flow Kit, following the manufacturer's instructions (BD, catalog number 559619). Briefly, cells were stained for extracellular antigens for 30 minutes on ice, fixed with Cytofix/Cytoperm (BD Biosciences, catalog number 554722) for 15 minutes, and then washed 3 times with PBS and incubated with intracellular antibody in 2% FBS in PBS for 30 minutes at room temperature. Analysis was performed on a FACSCanto II (BD).

For PB T cell staining, cells were labeled with V450-CD3 (BD Biosciences, 561389, 1:200), PE-CD4 (Biolegend, 100407, 1:200), BV605-CD8 (BD Biosciences, 563152, 1:200), APC/Cy7-CD44 (Biolegend, 103027, 1:200), FITC-CD62L (Biolegend, 104405, 1:200), and Alexa Fluor 647 CD45RA (BD Biosciences, 562763, 1:200). For B/NK cell staining, cells were labeled with V450-

CD3 (BD Biosciences, 561389, 1:200), Alexa Fluor 647 NK1.1 (Biolegend, 108719, 1:200), PE-CD122 (Biolegend, 105905, 1:200), and FITC-CD19 (Biolegend, 152403 1:200). Corresponding isotypes were used to confirm antibody staining efficiency and compensation controls were used to set gates. Effector memory T cells ($CD3^+CD4/8^+CD44^+CD62L^-$), naive T cells ($CD3^+CD4/8^+CD44^-CD62L^+$), cytotoxic T cells ($CD3^+CD8^+$), B cells ($CD3^-CD19^+$), and NK cells ($CD3^-CD19^-CD122^+NK1.1^+$) were analyzed using FlowJo analysis software version 10. Numbers of each PB population were calculated by multiplying the percentages of each subset by the total WBCs in each sample.

The thymi of 8- to 10-week-old $Kras^{nat/nat}$ mice and $Kras^{ex3op/ex3op}$ mice were harvested and pressed through a 70-μm cell strainer (Falcon) with the plunger of a 3-ml syringe to obtain a cell suspension. Cells were kept in cold analysis medium (PBS 1×, 0.1% BSA, and 2 mM EDTA) throughout the entire experiment. Thymocytes were then counted using a hemacytometer (Hausser Scientific) and viability was determined by trypan blue exclusion (Sigma-Aldrich). For early T cell progenitor analysis, 25×10^6 to 50×10^6 thymocytes were incubated with purified anti-CD4 (clone RM4-5, BD Biosciences) and anti-CD8 antibodies (clone 53-6.7, BD Biosciences), in addition to a cocktail of antibodies (anti-CD11b, anti-CD16/32, anti-B220, and anti-TER119) from a Dynabeads Untouched T cells kit (Invitrogen). After magnetic isolation with Dynabeads, lineage negative (lin^-) thymocytes were then counted and stained with the following conjugated antibodies: anti-CD45 FITC (30-F11), anti-B220 PerCPCy5.5 (RA3-6B2), anti-CD11b PerCP-Cy5.5 (M1/70), anti-Gr1 PerCP-Cy5.5 (RB6-8C5), anti-TER119 PerCP-Cy5.5, anti-CD25 PE-Cy7 (PC61), anti-CD117 APC (2B8) (all BD Biosciences); anti-CD4 APC-Cy7 (GK1.5), anti-CD8 BV711 (53-6.7), anti-CD3 BV510 (17A2), and anti-CD44 BV786 (IM7) (all BioLegend). For total thymocyte

analysis, 1×10^6 thymocytes were stained with the above-mentioned conjugated antibodies. For thymocyte maturation analysis, 1×10^6 total thymocytes were stained with the following conjugated antibodies: anti-CD45 PE (30-F11), anti-CD62L PerCP-Cy5.5 (MEL-14), anti-CD3 PE-Cy7 (17A2) (all BD Biosciences); anti-Qa2 FITC (695 H1-9-9), anti-CD8 APC-Cy7 (53-6.7), anti-CD69 BV510 (H1.2 F3), anti-CD4 BV605(GK1.5), and anti-CD24 BV711 (M1/69) (all BioLegend). Stained cells were then analyzed by flow cytometry (BD LSR Fortessa, BD Biosciences).

Phospho-flow cytometry

Following lineage depletion, BM cells were sorted for KSL cells. Cells were washed using IMDM with no FBS to serum starve for 30 minutes at 37°C. Subsequently, growth factor was added for 5 minutes prior to fixing by adding 10 volumes prewarmed Lyse/Fix buffer (BD Biosciences, 558049). Fixation was performed at 37°C for 10 minutes. Cells were washed in stain buffer (BD Biosciences, 554656), and then permeabilized with prechilled Perm Buffer III (BD Biosciences, 558050) on ice for 30 minutes. After washing with stain buffer 3 times, the cells were resuspended with the phospho-flow antibody at the recommended concentration overnight at 4°C prior to analysis. Antibodies were the following (all from BD Biosciences): Phosflow PE Mouse anti-Akt (pT308), 558275; Phosflow Alexa Fluor 647 Mouse anti-Akt (pS473), 560343; Phosflow Alexa Fluor 647 Mouse anti-S6 (pS244), 560465; Phosflow PE Mouse Anti-Stat5 (pY694), 612567; and PE Mouse Anti-ERK1/2 (pT202/pY204), 612566.

Immunohistochemical analysis

Freshly dissected femurs were decalcified using Surgipath Decalcifier II for 6 hours. Four-micron sections were created from formalin-fixed, paraffin-embedded blocks, using a rotary microtome, floated on a 49°C water bath, and mounted on a positively charged slide. All slides were baked overnight in a 65°C oven, stained with H&E, and then covered using resinous mounting medium. Paraffin-embedded sections were cut at 4-μm thickness and paraffin removed with xylene and rehydrated through graded ethanol. Images were acquired using a Zeiss Axio Imager M2.

Homing assay. *Kras*$^{nat/nat}$ mice (DsRed-negative) were irradiated with 900 cGy TBI. Using *Kras*$^{ex3op/ex3op}$*;DsRed* mice or *Kras*$^{nat/nat}$*;DsRed* mice as donors, we sorted BM KSL cells and injected 4×10^4 cells per recipient. We analyzed the BM at 18 hours after injection for DsRed$^+$ hematopoietic cells[75].

CFC assays

BM cells were plated in MethoCult GFM3434 (Stem Cell Technologies). Numbers of cells utilized and time of analysis are provided in the figure legends. Colonies were counted 14 days later, unless otherwise indicated by morphology. CFC assays (colony-forming unit–granulocyte monocyte [CFU-GM], burst-forming unit–erythroid [BFU-E], and CFU–granulocyte erythroid monocyte megakaryocyte [CFU-GEMM]) were performed as we have previously described[74].

LTC-IC assay

BM LTC-IC assay was performed as previously described[63], with minor modifications. Briefly, the unfractionated BM cells were plated on an irradiated (15 Gy) primary mouse stromal monolayer in 96-well plates containing 150 μl of M5300 medium (Stem Cell Technologies)

supplemented with 10–6 M hydrocortisone. The media were changed with half-fresh medium weekly until week 5 when the cells were harvested with trypsin and plated for CFCs in M3434 media (Stem Cell Technologies). The plates were evaluated for the presence of CFCs 10 days thereafter.

Radiation studies

Ten-week-old male *Kras*$^{ex3op/ex3op}$ mice or *Kras*$^{nat/nat}$ mice were treated with 750 cGy TBI using a Cesium-137 irradiator. Mice were monitored daily through day +30 and euthanized as per our approved animal use protocol, if necessary. Complete blood counts were measured using a Hemavet 950 instrument (Drew Scientific). For the limiting-dose BM transplantation experiment, 8-week-old male C57BL/6 mice received 850 cGy TBI followed by tail vein injection of 1×10^5 BM cells from *Kras*$^{ex3op/ex3op}$ mice or *Kras*$^{nat/nat}$ mice. Palbociclib or vehicle was administered intraperitoneally on day +5 and +6 at 85 mg/kg, dissolved in sodium lactate. For competitive transplants or chimeric mice generation, 950 cGy TBI was used and BM cells were injected 24 hours later. Mice were monitored daily through day +30 and euthanized per our animal use protocol, if necessary.

PCR

We performed gene expression analysis via qRT-PCR on populations of BM KSL cells. RNA was isolated using the Qiagen RNeasy Micro Kit. RNA was reverse transcribed into cDNA using an iScript cDNA synthesis kit and random hexamers. Real-time PCR analysis was performed using TaqMan Gene Expression assays (Life Technologies) on an Applied Biosystems QuantStudio 6

PCR Machine (Thermo Fisher Scientific). The primers used for TaqMan-based PCR are shown below. Data were normalized to GAPDH and littermate controls using the double-delta CT method. For CDK1, CCNE1, and B-MYB, the SYBR Green method was used. cDNA (20 ng) was used for qPCR with the SYBR Select Master Mix (Life Technologies). The sequences of the primers used for SYBR Green–based PCR are shown below. Values were normalized using GAPDH.

SYBR Green Primer Sequences

Gene	Forward Primer	Reverse Primer
GAPDH	TGGATTTGGACGCATTGGTC	TTTGCACTGGTACGTGTTGAT
CDK1	AGAAGGTACTTACGGTGTGGT	GAGAGATTTCCCGAATTGCAGT
B-MYB	TCTGGATGAGTTACACTACCAGG	GTGCGGTTAGGAAAGTGACTG
CCNE1	GTGGCTCCGACCTTTCAGTC	CACAGTCTTGTCAATCTTGGCA

TaqMan Primers

Gene	Assay ID
CCND1	Mm00432359_m1
CCND2	Mm00438070_m1
CDK8	Mm01223097_m1
p19 (CDKN2D)	Mm00486943_m1
p21 (CDKN1A)	Mm04205640_g1
p27 (CDKN1B)	Mm00438168_m1

Sanger Sequencing

DNA sequencing of *Ras* genes was performed by Laragen, Inc., and performed on an ABI 3730XL sequencer using BigDye on a 3.1 sequencing reaction. Five $Kras^{nat/nat}$ mice and 5 $Kras^{ex3op/ex3op}$ mice were tested using primers flanking exons containing codons 12, 13, and 61 in *Kras*, *Nras*, and *Hras*.

Statistics

Values are represented as means ± SEM or ± SD as noted in the figure legends. All comparisons were made using an unpaired 2-tailed Student's *t* test, unless otherwise indicated in the figure legends. A 2-sample equal variance with normal distribution was utilized and *P* values less than 0.05 were considered to be significant. GraphPad Prism 6.0 was used for all statistical analyses. All data were checked for normal distribution and similar variance between groups. Sample size for in vitro studies was chosen based on observed effect sizes and standard errors from prior studies. For animal studies, a power test was used to determine the sample size needed to observe a 2-fold difference in means between groups with 0.8 power using a 2-tailed Student's *t* test. All animal studies were performed using sex- and age-matched animals, with wild-type littermates as controls. Animal studies were performed without blinding of the investigator and no animals were excluded from the analysis. Statistical details of each experiment are described in the figure legends, including the numbers of replicates and *P* values from the Student's *t* test.

Study Approval

All animal studies were performed under UCLA animal care and use protocol 2014-021-13E (Principal Investigator, John Chute), approved by the UCLA Animal Care and Use Committee.

Chapter 6

References

1. Pershing NL, Lampson BL, Belsky JA, Kaltenbrun E, MacAlpine DM, Counter CM. Rare codons capacitate Kras-driven de novo tumorigenesis. *J Clin Invest*. 2015;125(1):222-233.

2. Ali M, Kaltenbrun E, Anderson GR, et al. Codon bias imposes a targetable limitation on KRAS-driven therapeutic resistance. *Nat Commun*. 2017;8:15617.

3. Pylayeva-Gupta Y, Grabocka E, Bar-Sagi D. RAS oncogenes: weaving a tumorigenic web. *Nat Rev Cancer*. 2011;11(11):761-774.

4. Stephen AG, Esposito D, Bagni RK, McCormick F. Dragging ras back in the ring. *Cancer Cell*. 2014;25(3):272-281.

5. Ahearn IM, Haigis K, Bar-Sagi D, Philips MR. Regulating the regulator: post-translational modification of RAS. *Nat Rev Mol Cell Biol*. 2011;13(1):39-51.

6. Hancock JF. Ras proteins: different signals from different locations. *Nat Rev Mol Cell Biol*. 2003;4(5):373-384.

7. Rocks O, Peyker A, Bastiaens PI. Spatio-temporal segregation of Ras signals: one ship, three anchors, many harbors. *Curr Opin Cell Biol*. 2006;18(4):351-357.

8. Quinlan MP, Settleman J. Isoform-specific ras functions in development and cancer. *Future Oncol*. 2009;5(1):105-116.

9. Cabezas-Wallscheid N, Buettner F, Sommerkamp P, et al. Vitamin A-Retinoic Acid Signaling Regulates Hematopoietic Stem Cell Dormancy. *Cell*. 2017;169(5):807-823.e819.

10. Zhang X, Su J, Jeong M, et al. DNMT3A and TET2 compete and cooperate to repress lineage-specific transcription factors in hematopoietic stem cells. *Nat Genet*. 2016;48(9):1014-1023.

11. Schubbert S, Bollag G, Lyubynska N, et al. Biochemical and functional characterization of germ line KRAS mutations. *Mol Cell Biol*. 2007;27(22):7765-7770.

12. Potenza N, Vecchione C, Notte A, et al. Replacement of K-Ras with H-Ras supports normal embryonic development despite inducing cardiovascular pathology in adult mice. *EMBO Rep*. 2005;6(5):432-437.

13. Serrano M, Lin AW, McCurrach ME, Beach D, Lowe SW. Oncogenic ras provokes premature cell senescence associated with accumulation of p53 and p16INK4a. *Cell*. 1997;88(5):593-602.

14. Hawley RG, Fong AZ, Ngan BY, Hawley TS. Hematopoietic transforming potential of activated ras in chimeric mice. *Oncogene*. 1995;11(6):1113-1123.

15. Dorrell C, Takenaka K, Minden MD, Hawley RG, Dick JE. Hematopoietic cell fate and the initiation of leukemic properties in primitive primary human cells are influenced by Ras activity and farnesyltransferase inhibition. *Mol Cell Biol*. 2004;24(16):6993-7002.

16. Braun BS, Tuveson DA, Kong N, et al. Somatic activation of oncogenic Kras in hematopoietic cells initiates a rapidly fatal myeloproliferative disorder. *Proc Natl Acad Sci U S A*. 2004;101(2):597-602.

17. MacKenzie KL, Dolnikov A, Millington M, Shounan Y, Symonds G. Mutant N-ras induces myeloproliferative disorders and apoptosis in bone marrow repopulated mice. *Blood*. 1999;93(6):2043-2056.

18. Sabnis AJ, Cheung LS, Dail M, et al. Oncogenic Kras initiates leukemia in hematopoietic stem cells. *PLoS Biol*. 2009;7(3):e59.

19. Li Q, Haigis KM, McDaniel A, et al. Hematopoiesis and leukemogenesis in mice expressing oncogenic NrasG12D from the endogenous locus. *Blood*. 2011;117(6):2022-2032.

20. Li Q, Bohin N, Wen T, et al. Oncogenic Nras has bimodal effects on stem cells that sustainably increase competitiveness. *Nature*. 2013;504(7478):143-147.

21. Van Meter ME, Diaz-Flores E, Archard JA, et al. K-RasG12D expression induces hyperproliferation and aberrant signaling in primary hematopoietic stem/progenitor cells. *Blood*. 2007;109(9):3945-3952.

22. Xu J, Haigis KM, Firestone AJ, et al. Dominant role of oncogene dosage and absence of tumor suppressor activity in Nras-driven hematopoietic transformation. *Cancer Discov*. 2013;3(9):993-1001.

23. Lyubynska N, Gorman MF, Lauchle JO, et al. A MEK inhibitor abrogates myeloproliferative disease in Kras mutant mice. *Sci Transl Med*. 2011;3(76):76ra27.

24. Tarnawsky SP, Kobayashi M, Chan RJ, Yoder MC. Mice expressing KrasG12D in hematopoietic multipotent progenitor cells develop neonatal myeloid leukemia. *J Clin Invest*. 2017;127(10):3652-3656.

25. Parikh C, Subrahmanyam R, Ren R. Oncogenic NRAS rapidly and efficiently induces CMML- and AML-like diseases in mice. *Blood*. 2006;108(7):2349-2357.

26. Gougopoulou DM, Kiaris H, Ergazaki M, Anagnostopoulos NI, Grigoraki V, Spandidos DA. Mutations and expression of the ras family genes in leukemias. *Stem Cells*. 1996;14(6):725-729.

27. Stirewalt DL, Appelbaum FR, Willman CL, Zager RA, Banker DE. Mevastatin can increase toxicity in primary AMLs exposed to standard therapeutic agents, but statin efficacy is not simply associated with ras hotspot mutations or overexpression. *Leuk Res*. 2003;27(2):133-145.

28. Zuber J, Radtke I, Pardee TS, et al. Mouse models of human AML accurately predict chemotherapy response. *Genes Dev*. 2009;23(7):877-889.

29. Poliseno L, Salmena L, Zhang J, Carver B, Haveman WJ, Pandolfi PP. A coding-independent function of gene and pseudogene mRNAs regulates tumour biology. *Nature*. 2010;465(7301):1033-1038.

30. Santos GC, Zielenska M, Prasad M, Squire JA. Chromosome 6p amplification and cancer progression. *J Clin Pathol*. 2007;60(1):1-7.

31. Damnernsawad A, Kong G, Wen Z, et al. Kras is Required for Adult Hematopoiesis. *Stem Cells*. 2016;34(7):1859-1871.

32. Chan G, Gu S, Neel BG. Erk1 and Erk2 are required for maintenance of hematopoietic stem cells and adult hematopoiesis. *Blood*. 2013;121(18):3594-3598.

33. Himburg HA, Harris JR, Ito T, et al. Pleiotrophin regulates the retention and self-renewal of hematopoietic stem cells in the bone marrow vascular niche. *Cell Rep*. 2012;2(4):964-975.

34. Himburg HA, Muramoto GG, Daher P, et al. Pleiotrophin regulates the expansion and regeneration of hematopoietic stem cells. *Nat Med*. 2010;16(4):475-482.

35. Himburg HA, Yan X, Doan PL, et al. Pleiotrophin mediates hematopoietic regeneration via activation of RAS. *J Clin Invest*. 2014;124(11):4753-4758.

36. Lampson BL, Pershing NL, Prinz JA, et al. Rare codons regulate KRas oncogenesis. *Curr Biol*. 2013;23(1):70-75.

37. Nakamura Y, Gojobori T, Ikemura T. Codon usage tabulated from international DNA sequence databases: status for the year 2000. *Nucleic Acids Res*. 2000;28(1):292.

38. Kong G, Chang YI, Damnernsawad A, et al. Loss of wild-type Kras promotes activation of all Ras isoforms in oncogenic Kras-induced leukemogenesis. *Leukemia*. 2016;30(7):1542-1551.

39. Staffas A, Karlsson C, Persson M, Palmqvist L, Bergo MO. Wild-type KRAS inhibits oncogenic KRAS-induced T-ALL in mice. *Leukemia*. 2015;29(5):1032-1040.

40. Signer RA, Magee JA, Salic A, Morrison SJ. Haematopoietic stem cells require a highly regulated protein synthesis rate. *Nature*. 2014;509(7498):49-54.

41. Bourne HR, Sanders DA, McCormick F. The GTPase superfamily: a conserved switch for diverse cell functions. *Nature*. 1990;348(6297):125-132.

42. Boguski MS, McCormick F. Proteins regulating Ras and its relatives. *Nature*. 1993;366(6456):643-654.

43. Tan PB, Kim SK. Signaling specificity: the RTK/RAS/MAP kinase pathway in metazoans. *Trends Genet*. 1999;15(4):145-149.

44. Harper JW, Elledge SJ, Keyomarsi K, et al. Inhibition of cyclin-dependent kinases by p21. *Mol Biol Cell*. 1995;6(4):387-400.

45. Xiong Y, Hannon GJ, Zhang H, Casso D, Kobayashi R, Beach D. p21 is a universal inhibitor of cyclin kinases. *Nature*. 1993;366(6456):701-704.

46. Chang F, Steelman LS, McCubrey JA. Raf-induced cell cycle progression in human TF-1 hematopoietic cells. *Cell Cycle*. 2002;1(3):220-226.

47. Rubin SM. Deciphering the retinoblastoma protein phosphorylation code. *Trends Biochem Sci*. 2013;38(1):12-19.

48. Lundberg AS, Weinberg RA. Functional inactivation of the retinoblastoma protein requires sequential modification by at least two distinct cyclin-cdk complexes. *Mol Cell Biol*. 1998;18(2):753-761.

49. Lam EW, Watson RJ. An E2F-binding site mediates cell-cycle regulated repression of mouse B-myb transcription. *Embo j*. 1993;12(7):2705-2713.

50. DeGregori J, Kowalik T, Nevins JR. Cellular targets for activation by the E2F1 transcription factor include DNA synthesis- and G1/S-regulatory genes. *Mol Cell Biol*. 1995;15(8):4215-4224.

51. Furukawa Y, Terui Y, Sakoe K, Ohta M, Saito M. The role of cellular transcription factor E2F in the regulation of cdc2 mRNA expression and cell cycle control of human hematopoietic cells. *J Biol Chem*. 1994;269(42):26249-26258.

52. Takizawa H, Fritsch K, Kovtonyuk LV, et al. Pathogen-Induced TLR4-TRIF Innate Immune Signaling in Hematopoietic Stem Cells Promotes Proliferation but Reduces Competitive Fitness. *Cell Stem Cell*. 2017;21(2):225-240.e225.

53. Bernitz JM, Kim HS, MacArthur B, Sieburg H, Moore K. Hematopoietic Stem Cells Count and Remember Self-Renewal Divisions. *Cell*. 2016;167(5):1296-1309.e1210.

54. Wilson A, Laurenti E, Oser G, et al. Hematopoietic stem cells reversibly switch from dormancy to self-renewal during homeostasis and repair. *Cell*. 2008;135(6):1118-1129.

55. Castellano E, Santos E. Functional specificity of ras isoforms: so similar but so different. *Genes Cancer*. 2011;2(3):216-231.

56. Parikh C, Subrahmanyam R, Ren R. Oncogenic NRAS, KRAS, and HRAS exhibit different leukemogenic potentials in mice. *Cancer Res*. 2007;67(15):7139-7146.

57. Meloche S, Pouyssegur J. The ERK1/2 mitogen-activated protein kinase pathway as a master regulator of the G1- to S-phase transition. *Oncogene*. 2007;26(22):3227-3239.

58. Shaulian E, Karin M. AP-1 in cell proliferation and survival. *Oncogene*. 2001;20(19):2390-2400.

59. Liu Y, Martindale JL, Gorospe M, Holbrook NJ. Regulation of p21WAF1/CIP1 expression through mitogen-activated protein kinase signaling pathway. *Cancer Res*. 1996;56(1):31-35.

60. Mende N, Kuchen EE, Lesche M, et al. CCND1-CDK4-mediated cell cycle progression provides a competitive advantage for human hematopoietic stem cells in vivo. *J Exp Med*. 2015;212(8):1171-1183.

61. Laurenti E, Frelin C, Xie S, et al. CDK6 levels regulate quiescence exit in human hematopoietic stem cells. *Cell Stem Cell*. 2015;16(3):302-313.

62. He S, Roberts PJ, Sorrentino JA, et al. Transient CDK4/6 inhibition protects hematopoietic stem cells from chemotherapy-induced exhaustion. *Sci Transl Med*. 2017;9(387).

63. Cheng T, Rodrigues N, Shen H, et al. Hematopoietic stem cell quiescence maintained by p21cip1/waf1. *Science*. 2000;287(5459):1804-1808.

64. Ichise T, Yoshida N, Ichise H. H-, N- and Kras cooperatively regulate lymphatic vessel growth by modulating VEGFR3 expression in lymphatic endothelial cells in mice. *Development*. 2010;137(6):1003-1013.

65. To LB, Levesque JP, Herbert KE. How I treat patients who mobilize hematopoietic stem cells poorly. *Blood*. 2011;118(17):4530-4540.

66. Arai Y, Kondo T, Yamazaki H, et al. Allogeneic unrelated bone marrow transplantation from older donors results in worse prognosis in recipients with aplastic anemia. *Haematologica*. 2016;101(5):644-652.

67. Cutler C, Kim HT, Sun L, et al. Donor-specific anti-HLA antibodies predict outcome in double umbilical cord blood transplantation. *Blood*. 2011;118(25):6691-6697.

68. Kanda J, Rizzieri DA, Gasparetto C, et al. Adult dual umbilical cord blood transplantation using myeloablative total body irradiation (1350 cGy) and fludarabine conditioning. *Biol Blood Marrow Transplant*. 2011;17(6):867-874.

69. Silberstein L, Goncalves KA, Kharchenko PV, et al. Proximity-Based Differential Single-Cell Analysis of the Niche to Identify Stem/Progenitor Cell Regulators. *Cell Stem Cell*. 2016;19(4):530-543.

70. Mercier FE, Sykes DB, Scadden DT. Single Targeted Exon Mutation Creates a True Congenic Mouse for Competitive Hematopoietic Stem Cell Transplantation: The C57BL/6-CD45.1(STEM) Mouse. *Stem Cell Reports*. 2016;6(6):985-992.

71. Chen JY, Miyanishi M, Wang SK, et al. Hoxb5 marks long-term haematopoietic stem cells and reveals a homogenous perivascular niche. *Nature*. 2016;530(7589):223-227.

72. Li Q, Bohin N, Wen T, et al. Oncogenic Nras has bimodal effects on stem cells that sustainably increase competitiveness. *Nature*. 2013;504(7478):143-147.

73. Himburg HA, Doan PL, Quarmyne M, et al. Dickkopf-1 promotes hematopoietic regeneration via direct and niche-mediated mechanisms. *Nat Med*. 2017;23(1):91-99.

74. Yan X, Himburg HA, Pohl K, et al. Deletion of the Imprinted Gene Grb10 Promotes Hematopoietic Stem Cell Self-Renewal and Regeneration. *Cell Rep*. 2016;17(6):1584-1594.

75. Christopherson KW, 2nd, Hangoc G, Mantel CR, Broxmeyer HE. Modulation of hematopoietic stem cell homing and engraftment by CD26. *Science*. 2004;305(5686):1000-1003.